

1 **The genomic landscape of intrinsic and acquired resistance to cyclin-
2 dependent kinase 4/6 inhibitors in patients with hormone receptor positive
3 metastatic breast cancer**

4
5 Authors:

6 Seth A. Wander^{1,2,3,4}

7 Ofir Cohen^{1,2,4}

8 Xueqian Gong^{1, 5}

9 Gabriela N. Johnson^{1,2,4}

10 Jorge Buendia-Buendia^{1,2,4}

11 Maxwell R. Lloyd^{1,2}

12 Dewey Kim^{1,2,4}

13 Flora Luo^{1,2,3,4}

14 Pingping Mao^{1,2,3,4}

15 Karla Helvie^{1,2}

16 Kailey J. Kowalski^{1,2,4}

17 Utthara Nayar^{1,2,3,4}

18 Adrienne G. Waks^{1,2,3,4}

19 Stephen Parsons⁵

20 Ricardo Martinez⁵

21 Lacey M. Litchfield⁵

22 Xiang S. Ye⁵

23 Chun Ping Yu⁵

24 Valerie M. Jansen⁵

25 John R. Stille⁵

26 Patricia S. Smith⁵

27 Gerard J. Oakley⁵

28 Quincy Chu⁶

29 Gerald Batist⁷

30 Melissa Hughes^{1,2}

31 Jill D. Kremer⁵

32 Levi A. Garraway^{1,2,3,4,5}

33 Eric P. Winer^{2,3}

34 Sara M. Tolaney^{2,3}

35 Nancy U. Lin^{2,3}

36 Sean Buchanan⁵

37 Nikhil Wagle^{1,2,3,4}

38
39 1. Center for Cancer Precision Medicine, Dana-Farber Cancer Institute,
40 Boston, MA

41 2. Department of Medical Oncology, Dana-Farber Cancer Institute, Boston,
42 MA

43 3. Harvard Medical School, Boston, MA

44 4. Broad Institute of MIT and Harvard, Cambridge, MA

45 5. Eli Lilly and Co., Indianapolis, IN

46 6. Cross Cancer Institute, Alberta, Canada

47 7. Segal Cancer Centre, Jewish General Hospital, McGill University,
48 Montreal, Canada

49

50 Running title:

51 Genomic mechanisms of CDK 4/6 inhibitor resistance in metastatic breast cancer

52

53 Key words: CDK 4/6, metastatic breast cancer, whole exome sequencing, aurora
54 kinase, retinoblastoma

55

56 *Address correspondence to:

57 Nikhil Wagle, MD

58 Department of Medical Oncology

59 Dana-Farber Cancer Institute

60 450 Brookline Ave, Dana 820

61 Boston, MA 02215

62 Phone: 617-632-6419

63 e-mail: nikhil_wagle@dfci.harvard.edu

64

65 [£]These authors contributed equally

66

67 **Competing Financial Interest Statement**

68 SAW has served as an advisor/consultant to Foundation Medicine (consulting);
69 Eli Lilly (consulting); Puma Biotechnology (consulting); and InfiniteMD
70 (consulting, equity) and receives institutional research funding from Genentech.
71 AGW receives institutional research funding from Genentech and MacroGenics.
72 QC receives institutional research funding from Abbvie, Amgen, Astra Zeneca,
73 Aurka, Boheringer Ingelheim, BMS, Celgene, Debio, Espanas, Eli Lilly, GSK,
74 Merck, Novartis, Roche, TP Therapeutics; as well as advisory fees and honoraria
75 from Abbvie, Astra Zeneca, Boehringer Ingelheim, BMS, Eli Lilly, Merck,
76 Novartis, Roche, Takeda. SMT has received institutional research support from
77 Merck, Bristol-Myers Squibb, Exelixis, Eli Lilly, Pfizer, Novartis, AstraZeneca,
78 Eisai, Nektar, Odeon, Sanofi, Immunomedics, Cyclacel, and Genentech; and
79 has served as a consultant/advisor for Genentech, Eli Lilly, Novartis, Pfizer,
80 Celldex, Paxman, Seattle Genetics, Nektar, Immunomedics, Nanostring, Daiichi-
81 Sankyo, Bristol-Meyers Squibb, Sanofi, Abbvie, Athenex, AstraZeneca, Eisai,
82 Puma, and Merck. NUL is a consultant for Puma Biotechnology, Seattle
83 Genetics, and Daichii Sankyo, and received institutional research funding from
84 Merck, Pfizer, Genentech, Array Biopharma, Novartis and Seattle Genetics. EPW
85 has served as a consultant/advisor for InfiniteMD, Genentech, and Eli Lilly. NW
86 was previously a stockholder and consultant for Foundation Medicine; has been
87 a consultant/advisor for Novartis and Eli Lilly; and has received sponsored
88 research support from Novartis and Puma Biotechnology. XG, SP, RM, LML,
89 XSY, CPU, GJO, VMJ, JRS, PSS, LAG, and SB were employees and
90 shareholders of Eli Lilly and Company at the time of manuscript preparation.
91 Except as indicated by the author affiliations, none of these entities had any role
92 in the conceptualization, design, data collection, analysis, decision to publish, or
93 preparation of the manuscript.

94

95 **Abstract**

96 Clinical resistance mechanisms to CDK4/6 inhibitors in HR+ breast cancer have
97 not been clearly defined. Whole exome sequencing of 59 tumors with CDK4/6i
98 exposure revealed multiple candidate resistance mechanisms including *RB1*
99 loss, activating alterations in *AKT1*, *RAS*, *AURKA*, *CCNE2*, *ERBB2*, and *FGFR2*,
100 and loss of ER expression. *In vitro* experiments confirmed that these alterations
101 conferred CDK4/6i resistance. Cancer cells cultured to resistance with CDK4/6i
102 also acquired *RB1*, *KRAS*, *AURKA*, or *CCNE2* alterations, which conferred
103 sensitivity to *AURKA*, *ERK*, or *CHEK1* inhibition. Besides inactivation of *RB1*,
104 which accounts for ~5% of resistance, seven of these mechanisms have not
105 been previously identified as clinical mediators of resistance to CDK4/6 inhibitors
106 in patients. Three of these—*RAS* activation, *AKT* activation, and *AURKA*
107 activation—have not to our knowledge been previously demonstrated
108 preclinically. Together, these eight mechanisms were present in 80% of resistant
109 tumors profiled and may define therapeutic opportunities in patients.

110

111 **Significance**

112 We identified eight distinct mechanisms of resistance to CDK4/6 inhibitors
113 present in 80% of resistant tumors profiled. Most of these have a therapeutic
114 strategy to overcome or prevent resistance in these tumors. Taken together,
115 these findings have critical implications related to the potential utility of precision-
116 based approaches to overcome resistance in many patients with HR+ MBC.

117 **Introduction**

118 The cyclin-dependent kinase 4/6 inhibitors (CDK4/6i) have entered widespread
119 use in both the first- and subsequent-line setting for patients with hormone-
120 receptor positive (HR+), human epidermal growth factor receptor 2 negative
121 (HER2-) metastatic breast cancer (MBC).^{1,2} Their application has resulted in
122 significant improvements in progression-free survival (PFS) and overall survival
123 (OS) for treatment-naïve and previously treated patients in combination with anti-
124 estrogens.³⁻⁹ Abemaciclib has shown efficacy as a single agent in endocrine-
125 refractory disease, and has been approved for use as monotherapy in pre-
126 treated patients with HR+/HER2- MBC.¹⁰ Despite these advances, HR+/HER2-
127 MBC remains a significant cause of morbidity and mortality. Many patients
128 demonstrate *de novo*, or intrinsic, resistance to these agents and, in those who
129 respond, acquired resistance and disease progression is unfortunately inevitable.

130

131 We have limited insight into the molecular pathways governing resistance to
132 CDK4/6i. Early development of these compounds indicated preferential efficacy
133 in luminal/Rb-positive cell lines.¹¹ Loss of Rb expression has been identified in
134 cellular models cultured to resistance in CDK4/6i.¹² Acquired *RB1* loss-of-
135 function mutations were identified in circulating tumor DNA (ctDNA) from three
136 patients following progression on CDK4/6i-based therapy.¹³ Analysis of ctDNA
137 from patients treated on the PALOMA-3 trial, which explored palbociclib with
138 fulvestrant versus fulvestrant alone in the second-line metastatic setting,
139 demonstrated rare *RB1* mutations that were uniquely present in the group

140 receiving palbociclib.¹⁴ *PIK3CA* and *ESR1* mutations were identified frequently
141 on both arms of the study, and neither has been well established as a predictive
142 biomarker.^{14,15} Recent analysis of ctDNA and tumors from the MONARCH-2
143 study, exploring abemaciclib and fulvestrant in patients with prior progression on
144 anti-estrogen therapy, suggested benefit from abemaciclib use regardless of
145 *PIK3CA* or *ESR1* status, though the magnitude of benefit was larger in mutant
146 patients.¹⁶ Despite lack of robust data supporting a role for PI3K, loss of the
147 *PTEN* tumor suppressor was recently noted in tumor samples with progression
148 on ribociclib, and was sufficient to promote resistance *in vitro*.¹⁷ Preclinically,
149 PDK1, another PI3K pathway effector, emerged from a kinome-wide screen in
150 HR+ cells as a potential mediator of resistance to CDK4/6i; targeting PDK1 or
151 PI3K prompted resensitization to CDK4/6i.¹⁸

152
153 Preclinical studies have also implicated overexpression of CDK6 and cyclin E2
154 (CCNE2) in mediating resistance.^{19,20} Increased expression of cyclin E1
155 (CCNE1) was associated with inferior response to palbociclib on PALOMA-3,
156 while the expression of cyclin D1, RB1, and CDK4 failed to demonstrate any
157 association.²¹ Targeted sequencing of tumor specimens from patients with HR+
158 MBC and CDK4/6i exposure suggested that regulation of CDK6 expression via
159 the FAT1 tumor suppressor could provoke resistance²² and CDK6 expression
160 may also be regulated via micro-RNA-dependent modulation of the TGF-B
161 pathway, altering sensitivity to CDK4/6i *in vitro* and in patients.²³

162

163 Prior work from our laboratory has implicated alterations in *ERBB2* and *FGFR2* in
164 mediating resistance to CDK4/6i *in vitro* and in patients.^{24,25} In addition,
165 amplification of *FGFR1*, identified via sequencing of ctDNA from MONALEESA-2
166 (ribociclib and anti-estrogen in the first-line metastatic setting), correlated with
167 reduced PFS and activation of FGFR1 provoked resistance *in vitro*.²⁶

168

169 Here we explore the genomic landscape of resistance to CDK4/6i via whole
170 exome sequencing of tumor biopsies. The landscape of resistance to CDK4/6i is
171 heterogeneous, with multiple potential mediators including biallelic *RB1*
172 disruption and activation of *AKT1*, *RAS*, *ERBB2*, *FGFR2*, Aurora Kinase A
173 (*AURKA*), and *CCNE2*. Modification of HR+ breast cancer cells, via CRISPR-
174 mediated knockout or lentiviral overexpression, corroborates the candidate
175 mechanisms of resistance identified by tumor sequencing. Cells cultured to
176 resistance in the presence of CDK4/6i demonstrate concordant alterations in
177 *RB1*, *AURKA*, and *CCNE2* expression along with RAS/ERK activation and
178 demonstrate enhanced sensitivity to novel targeted therapies. In one patient with
179 HR+/HER2- MBC that progressed on first-line CDK4/6i, *AURKA* inhibition
180 provoked prolonged disease control in a phase I clinical trial. These results shed
181 new light on the diverse landscape of genomic alterations that drive resistance to
182 CDK4/6i in HR+/HER2- MBC and provide preclinical and translational rationale
183 for novel strategies to circumvent and overcome resistance.

184

185 **Results**

186 **The genomic landscape of intrinsic and acquired CDK4/6i resistance**

187 We identified patients with HR+/HER2- MBC who were treated with CDK4/6i with
188 or without an anti-estrogen and provided metastatic tumor biopsies as part of an
189 IRB-approved tissue collection protocol.²⁷ We classified samples as reflecting
190 sensitivity, intrinsic resistance, or acquired resistance (Figure 1A). Sensitive
191 biopsies were defined as baseline samples obtained within 120 days prior to, or
192 up to a maximum of 31 days after, CDK4/6i initiation in a patient with subsequent
193 clinical benefit (defined as radiographic response or stable disease >6 months).
194 Biopsies reflecting intrinsic resistance were obtained within 120 days prior to or
195 anytime after CDK4/6i initiation in patients without evidence of clinical benefit
196 (defined as progression on the first interval restaging study or stable disease <6
197 months). Biopsies reflecting acquired resistance were obtained from patients
198 who had experienced clinical benefit with CDK4/6i and had an available biopsy
199 specimen within 31 days prior to progression or at any time thereafter.

200

201 WES was successfully performed on 59 biopsies from 58 patients within the
202 appropriate exposure window to be assigned a phenotype and with sufficient
203 clinical data to define response (Supplemental Table 1). This included 18
204 sensitive biopsies, 28 intrinsic resistance biopsies, and 13 acquired resistance
205 biopsies. The majority of patients (55, 94.8%) received standard combinations of
206 an aromatase inhibitor or fulvestrant and a CDK4/6 inhibitor. 49 patients (84.5%)
207 received a palbociclib-based regimen, including 28 patients (48.3%) with an

208 aromatase inhibitor and 20 patients (34.5%) with fulvestrant. The mean duration
209 of therapy was 316 days (range 43-1052). Patients received an average of 1.5
210 lines of therapy in the metastatic setting (range 0-7) and 30 patients (51.7%) had
211 prior anti-estrogen exposure in the metastatic setting. Additional clinical
212 parameters are described in Supplemental Table 2.

213

214 Whole exome sequencing of all 59 samples demonstrated a number of genomic
215 alterations in genes implicated in HR+ breast cancer (*ESR1*, *PIK3CA*, *CCND1*,
216 *FGFR1*, *TP53*) as well as additional cancer genes and putative resistance
217 mediators (*RB1*, *ERBB2*, *FGFR2*, *AKT1*, *KRAS*, *HRAS*, *NRAS*, among others)
218 (Figure 1B, Supplemental Table 3). Many of these alterations were enriched in
219 resistant samples and not present or relatively infrequent in sensitive samples,
220 suggesting they might be contributing to resistance (Figure 1B; Supplemental
221 Figure 1; Supplemental Table 4). In addition to these genomic differences, three
222 patients with resistant tumor biopsies demonstrated loss of ER expression in the
223 metastatic drug-resistant tumor (measured by immunohistochemistry); all
224 patients were known to be ER+ at the time of metastatic diagnosis.

225

226 While isolated amplification events were identified in a variety of cancer genes
227 (Supplemental Table 4), amplification events in aurora kinase A were observed
228 as occurring more frequently in resistant samples as compared with sensitive (0
229 in sensitive, 26.8% in resistant; 0.0081, Welch test) (Figure 1C). While only
230 moderate magnitude AURKA amplifications were seen among the resistant

231 tumors, in The Cancer Genome Atlas (TCGA) study, even low AURKA
232 amplification in primary HR+ breast cancer samples resulted in a statistically
233 significant increase in gene expression (Supplementary Figure 2), suggesting
234 that the degree of AURKA amplification observed in the CDK4/6i-resistant cohort
235 is likely to have a meaningful effect on gene expression and protein level.

236

237 Based on prior preclinical studies and known biology, we hypothesized that the
238 following eight specific categories of alterations that were enriched in the
239 resistant tumors were contributing to CDK4/6i resistance: biallelic disruption of
240 *RB1*, activating mutation and/or amplification of *AKT1*, activating mutations in
241 *KRAS/HRAS/NRAS*, activating mutations and/or amplification of *FGFR2*,
242 activating mutations in *ERBB2*, amplification of *CCNE2*, amplification of AURKA,
243 and loss of ER.

244

245 In total, 33 out of the 41 resistant biopsies (80.5%) had genomic alterations in at
246 least one of these 8 potential resistance mechanisms, as compared to 3 of the 18
247 sensitive biopsies (Figure 1D, Supplemental Table 5). Consistent with prior
248 reports, biallelic disruption in *RB1* was exclusively present in resistant samples
249 and occurred in a minority of resistant biopsies (n=4/41, 9.8%). We identified
250 diverse mechanisms of biallelic *RB1* disruption across the affected patients. In all
251 examples, a single copy loss was noted in the presence of a point mutation,
252 splice site alteration, or frameshift event in the second allele.

253

254 AKT1 alterations were identified in five resistant biopsies (n=5/41, 12.2%),
255 including both mutational events and amplifications. A single sensitive biopsy
256 also demonstrated an activating AKT1 alteration (n=1/18, 5.6%).

257

258 Diverse RAS-pathway activating events were observed in four CDK4/6i-resistant
259 cases (n=4/41, 9.8%) including canonical activating mutations in *KRAS* G12D, a
260 pathogenic mutation in *KRAS* Q61L,²⁸ a mutation in *HRAS* K117N,²⁹ and high
261 focal amplification in *NRAS* (Figure 1B). There were no instances of RAS-altered
262 tumors with a sensitive phenotype.

263

264 Amplification events in AURKA were identified in eleven resistant biopsies
265 (n=11/41, 26.8%), including examples of both intrinsic and acquired resistance
266 (n=7 and n=4, respectively). There were no sensitive biopsies with AURKA
267 amplification.

268

269 There were six instances (n=6/41, 14.6%) of CCNE2 amplification identified
270 across the resistant cohort (Figure 1B). A single sensitive biopsy with a CCNE2
271 alteration was identified (n=1/18, 5.6%).

272

273 FGFR2 alterations were noted in three resistant biopsies (all with intrinsic
274 resistance) (n=3/41, 7.3%), while activating mutations or amplification of ERBB2
275 was noted in five resistant biopsies (n=5/41, 12.2%). A single sensitive biopsy
276 with an ERBB2 alteration was also identified (n=1/18, 5.6%).

277

278 With respect to ER signaling, three resistant biopsy samples exposed to CDK4/6i
279 and an anti-estrogen demonstrated loss of ER expression via IHC (n=3/41,
280 7.3%); there were no patients with ER loss among the sensitive tumor samples
281 (Figure 1B; Supplemental Table 5). These results support pre-clinical work
282 suggesting CDK4/6i was predominantly effective in HR+ luminal cell lines while
283 HR- basal cell lines demonstrated frequent intrinsic resistance.¹¹

284

285 Enrichment in *ESR1* mutations was appreciated amongst resistant tumors
286 (n=14/41, 34.1%; Supplemental Table 4) compared to sensitive tumors (n=3/18,
287 16.7%). *ESR1* mutations among sensitive tumors occurred exclusively in patients
288 receiving fulvestrant and were not found in patients who achieved clinical benefit
289 with CDK4/6i and an aromatase inhibitor, as would be expected (Supplementary
290 Figure 1).³⁰ These results support the notion that *ESR1* mutations are frequently
291 acquired during the development of endocrine resistance, while also suggesting
292 that they are not sufficient to drive simultaneous resistance to CDK4/6i.

293

294 Notably, mutational events in *PIK3CA* occurred frequently in both sensitive
295 (n=8/18, 44.4%) and resistant (n=18/41, 43.9%) specimens, suggesting that
296 *PI3KCA* is unlikely to be a marker of resistance. Copy number gains in *FGFR1*
297 were also noted amongst both sensitive (n=4/18, 22.2%) and resistant biopsies
298 (n=4/41, 9.8%).

299

300 Systematic differences in the relative proportion of these alterations were not
301 apparent when comparing the intrinsic and acquired resistance subgroups,
302 although the power of this analysis is limited by sample size (Figure 1D,
303 Supplemental Table 4).

304

305 **Evolutionary dynamics in acquired CDK4/6i resistance**

306 Matched pre- and post-treatment samples were available from seven patients
307 who experienced acquired resistance to CDK4/6i. We compared the WES from
308 the paired pre-treatment and post-treatment samples and performed an
309 evolutionary analysis to evaluate clonal structure and dynamics, including
310 changes in mutations and copy number. We established the evolutionary
311 classification of each mutation to distinguish events that were acquired or
312 enriched in clones that are dominant in the post-progression tumor, as compared
313 with the pre-treatment counterpart (Figure 2, Supplemental Table 6).

314

315 Potential drivers of resistance that are observed in evolutionary acquired clones
316 included a biallelic *RB1* disruption (Figure 2A), an *AKT1* amplification (Figure
317 2B), an *AKT1* activating mutation (Figure 2D), and an *ESR1* activating mutation
318 (Figure 2G).

319

320 In the patient with biallelic *RB1* disruption and an available matched pair for
321 exome analysis, the pre-treatment specimen demonstrated a single copy deletion
322 in *RB1*. Two separate post-progression biopsy samples demonstrated unique

323 alterations in the second copy of *RB1*, suggesting convergent evolution toward a
324 common mechanism of resistance within the same tumor ecosystem (Figure 2A).

325

326 Genomic diversity was also observed in various mechanisms of AKT activation.

327 In two patients with matched pre/post-treatment exome pairs, we observed
328 acquisition of a pathogenic *AKT1* point mutation (*W80R*)³¹⁻³³ (Figure 2D) and
329 acquisition of an *AKT1* copy-number amplification (Figure 2B). Taken together,
330 these cases suggest that cancer clones with activated AKT by either pathogenic
331 mutation or high copy-number can confer selective advantage under CDK4/6i
332 treatment.

333

334 In four of these pairs, the mechanism of acquired resistance remains unclear.
335 We did not identify any instances of acquired AURKA overexpression, RAS
336 activation, or CCNE2 amplification, though the analysis was limited by number of
337 available matched pairs.

338

339 **Clinical case histories of patients with CDK4/6 inhibitor resistance**

340 Figure 3 illustrates the clinical details of selected patients with intrinsic and
341 acquired resistance to CDK4/6i and putative driver alterations. These include four
342 instances of biallelic *RB1* disruption (Figure 3A), three patients with *AKT1*
343 activation (Figure 3B), three with RAS activation (Figure 3C), and three with high
344 CCNE2 amplification (Figure 3D).

345

346 Supplemental Figure 3 illustrates the three sensitive biopsy counter-examples: a
347 single instance of AKT1 activation (Supplemental Figure 3A), a patient with low-
348 level CCNE2 amplification (Supplemental Figure 3B), and a single ERBB2
349 alteration, all with clinical benefit on CDK4/6i (Supplemental Figure 3C).

350

351 Given the prominent (or exclusive) enrichment of *RB1* disruption, *AKT1*
352 activation, RAS mutation, *AURKA* amplification, and *CCNE2* amplification within
353 samples demonstrating resistance to CDK4/6i, we opted to pursue additional
354 molecular validation of these targets. Prior work from our group and others
355 implicating *FGFR* pathway and *ERBB2* activation in CDK4/6i resistance have
356 been reported elsewhere.²⁴⁻²⁶

357

358 **Candidate alterations provoke resistance to CDK4/6i and anti-estrogens in**
359 **vitro**

360 T47D and MCF7 HR+/HER2- breast cancer cells were utilized to explore whether
361 these five genetic alterations confer resistance to CDK4/6i *in vitro*. *AKT1*, *KRAS*
362 *G12D*, *AURKA*, and *CCNE2* were overexpressed via lentiviral transduction; *RB1*
363 was inactivated via CRISPR-mediated knockout (Figure 4A; Supplemental Figure
364 4A). The impact of these alterations on susceptibility to CDK4/6 inhibitors was
365 examined. Consistent with sequencing results, all alterations were sufficient to
366 cause resistance to either palbociclib or abemaciclib in T47D cells (Figure 4B-F).
367 Corresponding IC50 estimates for each dose-response curve are provided
368 (Supplemental Table 7). Similar results were obtained in MCF7 cells

369 (Supplemental Figure 3), though AURKA did not provoke resistance to CDK4/6i
370 in this cell line, suggesting that context dependence may explain differences
371 between cell lines, as with biopsies.

372

373 Given that most patients in the clinic are treated with a combination of CDK4/6i
374 and an anti-estrogen, we also explored sensitivity to fulvestrant (Supplemental
375 Figure 5). Cells lacking RB1 were only minimally resistant to fulvestrant
376 monotherapy in both T47D and MCF7. Both AKT1 and CCNE2 overexpression
377 conveyed resistance to fulvestrant in T47D and MCF7. Both KRAS G12D and
378 AURKA overexpression provoked significant resistance to fulvestrant in T47D
379 cells and but not in MCF7 cells.

380

381 Taken together, these results underscore the biological complexity related to the
382 emergence of clinical resistance to these drug combinations both *in vitro* and in
383 patients. They suggest that the resistance mechanisms identified in patient
384 samples may provoke differential resistance to the CDK4/6- and estrogen-based
385 components of the treatment regimen, and that these effects may depend upon
386 additional cell-specific features.

387

388 **Resistance mediators arise independently during culture to resistance and**
389 **define new dependencies *in vitro***

390 Given the results identified via exogenous manipulation of the mediators
391 described above, we sought to explore resistance to CDK4/6i via orthogonal

392 platforms in the laboratory. The HR+ cell lines T47D, MCF7, and MDA-MB-361
393 were cultured to resistance in the presence of increasing doses of palbociclib or
394 abemaciclib. To examine whether the putative drivers identified in patients were
395 also responsible for resistance under selection *in vitro*, we characterized the
396 resistant derivatives for levels of retinoblastoma protein, aurora kinase, cyclin E2
397 and for activated effectors of KRAS or AKT1 (Figure 5A).

398

399 Many of the putative resistance drivers identified via patient sequencing emerged
400 spontaneously under selective pressure *in vitro*. 361-AR-1 (a derivative of MDA-
401 MB-361 cells cultured to resistance in abemaciclib) was found to have an
402 oncogenic KRAS G12V mutation (data not shown) and demonstrated increased
403 ERK activation (Figure 5A). Proteomic analysis showed activation of multiple
404 MAPK pathway components, including ERK, MEK and RSK (Supplemental
405 Figure 6). T47D-AR-1 (a derivative of T47D cells cultured to resistance in
406 abemaciclib) demonstrated decreased RB1 along with increased AURKA and
407 pERK (Figure 5A). 361-PR-1 (a derivative of MDA-MB-361 cells cultured to
408 resistance in palbociclib) demonstrated increased AURKA and CCNE2 protein
409 levels (Figure 5A). Finally, MCF7-PR-1 (a derivative of MCF7 cells cultured to
410 resistance in palbociclib) demonstrated increased expression of CCNE2 (Figure
411 5A). All derivative cell lines were confirmed to be resistant to abemaciclib
412 compared with their parental counterparts (Figure 5B).

413

414 Therapeutic approaches are suggested by alterations identified in patient tumor
415 specimens and cell lines cultured to resistance (Figure 5C). 361-AR-1 cells
416 demonstrated increased KRAS/ERK activity and enhanced sensitivity to
417 LY3214996, a selective ERK inhibitor. Both AURKA-amplified and RB1-low cells
418 (T47D-AR-1 and 361-PR-1) were highly sensitive to LY3295668, a novel and
419 selective AURKA inhibitor that has previously been reported to show synthetic
420 lethality with RB1 loss.³⁴ Finally, cancers with high cyclin E and CDK2 activation
421 have been reported to be dependent on CHEK1.³⁵ CCNE2-amplified cells
422 (MCF7-PR-1) were highly sensitive to prexasertib, a CHEK1 inhibitor.
423 Corresponding IC50 values for CDK4/6i and targeted agent treatment for these
424 cell lines are included in Supplemental Table 8.

425
426 When compared to tumor sequencing results from patients with progression on
427 CDK4/6i, the spontaneous emergence of corresponding alterations *in vitro* lends
428 further support to the roles RB1 loss, RAS activation, CCNE2 overexpression,
429 and AURKA overexpression may play in mediating resistance. That these
430 alterations arose in parallel in different cancer cell lines (akin to different patients)
431 also supports the earlier observation that cellular context may dictate which
432 alterations arise under selective pressure via CDK4/6i. These results suggest
433 that, in the presence of specific driver alterations in resistant tumor cells, unique
434 dependencies may emerge which could inform novel therapeutic strategies.

435

436 **AURKA inhibition resulted in prolonged clinical benefit in a patient with**
437 **HR+/HER2-, RB1+ MBC following progression on CDK4/6i-based therapy**

438 LY3295668, the same AURKA specific inhibitor utilized *in vitro* to demonstrate a
439 new dependence on AURKA in MDA-MB-361 and T47D cells cultured to
440 resistance in CDK4/6i (Figure 5B, C), has entered early-stage clinical trials
441 (NCT03092934).

442

443 As a proof-of-concept example, we provide the case history of a patient with
444 locally advanced HR+/HER2- breast cancer treated on the trial. She had
445 chemotherapy and adjuvant tamoxifen prior to metastatic recurrence; at that
446 time, she was treated with first-line palbociclib and letrozole (Figure 6A). After
447 prolonged clinical benefit on this regimen (>3 years), she progressed and
448 enrolled on study with LY3295668. Her first restaging studies demonstrated
449 disease stability, which persisted for approximately 11 months (Figure 6A, top).
450 Immunohistochemical staining of her pre-treatment liver biopsy following
451 progression on CDK4/6i demonstrated high levels of the proliferative marker Ki67
452 and high RB1 protein expression (Figure 6A, bottom), suggesting the mechanism
453 of sensitivity to AURKA inhibition was not due to Rb loss. Sufficient additional
454 biopsy material was not available for further sequencing or IHC-based analysis at
455 the time of this writing. Our results lead us to speculate that sensitivity to AURKA
456 inhibition in this patient could be due to alternative resistance mechanisms, such
457 as AURKA amplification.

458 **Discussion**

459 CDK4/6 inhibitors, in combination with an anti-estrogen, have emerged as the
460 standard of care for HR+/HER2- MBC. Despite widespread use, we have limited
461 understanding of the mechanisms governing resistance and deciphering that
462 landscape constitutes a critically important unmet need. To our knowledge, we
463 provide the first analysis based upon whole exome sequencing of sensitive and
464 resistant tumor tissues in a diverse cohort of patients who received CDK4/6i. This
465 effort confirmed previous reports implicating rare events in RB1 while also
466 revealing novel mediators of resistance including AKT1, RAS family oncogenes,
467 AURKA, CCNE2, and ER loss. Prior work from our group and others identified
468 mutational events in ERBB2²⁵ and the FGFR pathway^{24,26,36} in driving resistance.
469 *In vitro* experiments confirm that AKT1, KRAS G12D, AURKA, and CCNE2
470 confer resistance to CDK4/6i. RB1 downregulation, RAS/ERK activation, AURKA
471 overexpression, and/or CCNE2 overexpression emerged spontaneously with
472 prolonged CDK4/6i exposure, lending further support to their putative role as
473 resistance effectors. These alterations correspond with the emergence of novel
474 dependencies *in vitro*, providing therapeutic rationale for new targeted strategies
475 in the clinic (Figure 6B). Finally, we provide an example of sustained clinical
476 benefit with a novel AURKA inhibitor in a patient with HR+/HER2- MBC following
477 progression on CDK4/6i.

478

479 Despite its central role downstream of CDK4/6, alterations in RB1 were observed
480 only in a minority of patients who developed resistance to CDK4/6i. Anecdotal

481 evidence of acquired alterations in RB1 at the time of progression was provided
482 via ctDNA sequencing in three patients with exposure to CDK4/6i.¹³ ctDNA
483 analysis from 195 patients treated on the PALOMA-3 study with fulvestrant and
484 palbociclib also demonstrated rare RB1 alterations (~5%), uniquely enriched in
485 the palbociclib-containing arm.¹⁴ Relatively frequent driver alterations in *PIK3CA*
486 and *ESR1* were also identified, though occurred in both treatment groups on
487 PALOMA-3. These results were consistent with a recent study in which pre-
488 treatment biopsies were subjected to targeted sequencing; alterations in RB1
489 were again rare (~3%) and were associated with significantly impaired PFS on
490 CDK4/6i.²² Our data supports the notion that RB1 alterations occur in a minority
491 of CDK4/6i-resistant patients (4/41, ~9.8%) and we provide new insight into
492 diverse mechanisms of biallelic disruption. In a single patient with multiple pre-
493 and post-treatment biopsies, two distinct mechanisms of biallelic inactivation
494 were identified in separate post-progression biopsies, demonstrating convergent
495 evolution under selective pressure for tumors with single copy loss *in vivo*. These
496 findings were supported by culture to resistance experiments, in which multiple
497 cell lines downregulated RB1 expression under selective pressure. While the rate
498 of genomic RB1 disruption in tumor samples appears to be low following
499 progression, additional non-genomic events may be missed by targeted or
500 exome-based sequencing (such as methylation, mutations in regulatory regions,
501 or post-translational modification). These possibilities warrant additional study.

502

503 Prior efforts suggested that common alterations in *CCND1*, *PIK3CA*, and *ESR1*
504 did not impact PFS on CDK4/6i. We did not find an association between
505 *CCND1*, *PIK3CA*, or *ESR1* alterations and CDK4/6i resistance in tumor
506 specimens. Of note, alterations in *TP53* were enriched in CDK4/6i resistant
507 biopsies. Mutant *TP53* is not sufficient to promote resistance to CDK4/6i *in vitro*
508 as MCF7 (*TP53* wild-type) and T47D (*TP53* mutant) are both sensitive at
509 baseline. Enrichment of *TP53* mutation in resistant specimens may result from
510 heavier pre-treatment (including chemotherapies), may be permissive for the
511 development of other resistance-promoting alterations, or may cooperate with
512 secondary alterations to drive CDK4/6i resistance *in vivo*. The role of *TP53* in
513 CDK4/6i resistance remains an active area of research in the laboratory.

514

515 Several lines of evidence suggest CDK6 as a potential mechanism of resistance
516 to CDK4/6 inhibitors.¹⁹ While clinical studies have not identified any examples of
517 CDK6 alterations in resistant samples, a recent study that performed targeted
518 sequencing in 348 tumor specimens obtained prior to treatment with CDK4/6i
519 demonstrated that loss of function mutations in the *FAT1* tumor suppressor
520 resulted in resistance to CDK4/6i. Interestingly, *FAT1* was shown to result in
521 upregulation of CDK6 expression via the Hippo pathway *in vitro*.²² Finally, recent
522 work from our institution demonstrated that micro-RNAs modulate CDK6
523 expression via the TGF-B pathway to alter sensitivity to CDK4/6i *in vitro*.²³
524 Increased expression of the implicated miRNA (432-5p) correlated with
525 resistance in a subset of the breast cancer patients exposed to CDK4/6i from the

526 cohort analyzed here.²³ In our study, we did not find examples of activating
527 events in CDK6, nor did we identify *FAT1* alterations amongst resistant samples.
528 Deletion and truncation mutations in *FAT1* appear to be extremely rare (reported
529 in 6 of 348 patients in *Li et al*).²² Given their very low frequency and our sample
530 size (n=58 patients), our study was likely not sufficiently powered to identify this
531 rare event.

532

533 Unlike ctDNA-based targeted sequencing reported from the PALOMA-3 study,
534 the cohort analyzed here represents, to our knowledge, the first analysis based
535 upon whole exome sequencing from clinically annotated biopsies reflecting a
536 diverse group of patients with exposure to multiple CDK4/6i-based regimens. In
537 addition to expected alterations in RB1, we identified a heterogeneous landscape
538 of resistance, in which a variety of rare driver events span a diverse spectrum of
539 potential mediators. We confirm enrichment of activating mutations in *ERBB2*
540 and amplification events in *FGFR2* in resistant patients, and both pathways
541 provoke resistance to anti-estrogens and CDK4/6i *in vitro*.^{24-26,36} We present, to
542 our knowledge, the first evidence implicating *AKT1*, *RAS*, and *AURKA* in
543 mediating resistance to CDK4/6i in patients. Targeted sequencing of ctDNA via
544 samples from PALOMA-3 also identified rare events in *ERBB2*, *AKT1*, *KRAS*,
545 and *FGFR2* which were both acquired and maintained at progression, however
546 this analysis was limited by lack of insight into the clinical response phenotype of
547 these samples.¹⁴ We would hypothesize that “maintained” alterations identified in
548 the context of that study represent instances of early- or intrinsic resistance while

549 “acquired” alterations are more likely to arise in patients with transient response
550 or clinical benefit from CDK4/6i. CCNE2 and AURKA did not emerge as potential
551 resistance mediators in that study, likely due to lack of insight into copy number
552 alterations as a result of the sequencing methodology.

553

554 More recent correlative analyses from PALOMA-3 suggested that CCNE1
555 expression is associated with inferior outcome for patients receiving palbociclib.²¹
556 While we did not see examples of CCNE1 amplification in this cohort, we do
557 provide, to our knowledge, the first evidence that CCNE2 amplification is also
558 associated with the resistant phenotype. Of note, given its proximity to the
559 centromere, copy number analysis of CCNE1 via WES is technically challenging
560 and this may have resulted in under-estimation of amplification events in this
561 gene.

562

563 While all of these mediators provoked resistance to CDK4/6i *in vitro*, in specific
564 instances there were cell-line-dependent differences in their ability to circumvent
565 CDK4/6i. This notion of context-specificity is supported by several isolated
566 counter-examples in patients, in which putative resistance mediators were found
567 to occur in individual patients who derived at least transient clinical benefit from
568 CDK4/6i. These findings are also consistent with the spontaneous emergence of
569 distinct resistance mediators in specific cell lines – for example, RAS/ERK-
570 activated and AURKA-amplified cells emerged in MDA-MB-361 but not in MCF7,
571 and exogenous overexpression of AURKA could not provoke resistance in

572 MCF7. The situation is further complicated by variation in anti-estrogen
573 resistance *in vitro*. As an example, AKT1 overexpression may be sufficient to
574 provoke resistance to both CDK4/6i and fulvestrant, while alterations in RB1 may
575 require a second cooperative event to overcome the anti-estrogen component of
576 the regimen (such as *ESR1* alteration). These nuances underscore the
577 complexity of modeling resistance to therapeutic combinations *in vitro* and
578 highlight the need for additional studies to explore context-specific factors, which
579 might dictate the emergence of resistance with a potential driver of interest.

580

581 The majority of alterations identified in our clinical cohort, and confirmed *in vitro*,
582 are amenable to therapeutic intervention via emerging agents (Figure 6B). These
583 results suggest that a non-selective regimen is unlikely to yield reliable clinical
584 benefit, while a precision-based approach, informed by the underlying genomic
585 findings at progression, could guide selection of therapy in CDK4/6i-resistant
586 patients. RAS-activated cells that emerged under selective pressure with
587 CDK4/6i were highly sensitive to LY3214996, a selective ERK inhibitor. The
588 CHEK1 kinase plays well-established roles in regulating cell cycle progression in
589 the setting of DNA damage.³⁷ Cancer cells with replication stress caused by
590 activated CDK2 appear to be particularly sensitive to Chk inhibitors³⁸ and CCNE1
591 amplification has been linked to CHEK1 dependence.³⁵ HR+ cells expressing
592 high levels of CCNE2 demonstrated enhanced sensitivity to prexasertib, a
593 CHEK1 inhibitor that has been well tolerated in human patients with early
594 evidence suggesting clinical efficacy in a phase I study.³⁹

595

596 The aurora kinases regulate organization of the mitotic spindle and cell cycle
597 progression.⁴⁰ AURKA overexpression in breast cancer has been associated with
598 an ER-low/basal phenotype.⁴¹ AURKA was previously implicated in mediating
599 endocrine resistance via SMAD-dependent downregulation of ER-alpha
600 expression.⁴² Alisertib, an oral AURKA inhibitor, was well tolerated in HR+ MBC
601 patients when combined with fulvestrant, and anti-tumor activity was appreciated
602 in a phase I trial.⁴³ A randomized phase II study of this combination has
603 completed accrual (NCT02860000). We demonstrate that HR+ cells cultured to
604 resistance in CDK4/6i can demonstrate downregulation of RB1 or increased
605 expression of AURKA, both of which are associated with increased sensitivity to
606 LY3295668, a novel selective AURKA inhibitor. In screens to identify synthetic
607 lethal interactions with an RB1 mutation in lung and other cancers, the aurora
608 kinases emerged as key targets, and LY3295668 provoked tumor regression in
609 xenograft models of RB1-null small cell lung cancer.^{34,44} We provide the first
610 evidence supporting AURKA as a mediator of resistance to CDK4/6i *in vitro* and
611 in tumor samples. Furthermore, in a patient with HR+ MBC who progressed after
612 a prolonged course of CDK4/6i-based therapy (analogous to our translational
613 culture-to-resistance experiment *in vitro*), subsequent treatment on a phase I trial
614 with LY3295668 was well tolerated and prompted prolonged clinical benefit. This
615 patient had high RB1 protein expression at the time of therapy initiation,
616 suggesting that her response was not governed by RB1 loss. Based upon these
617 translational insights, a phase I study exploring the utility of LY3295668 in

618 patients with HR+ MBC following progression on CDK4/6i was recently initiated
619 (NCT03955939).

620

621 Although one can consider targeting each individual resistance mechanism
622 directly, it may also be possible to target a smaller number of resistance “nodes”
623 or pathways upon which multiple resistance effectors converge. We previously
624 showed that *ERBB2* mutations and alterations in FGFR1/FGFR2 activate the
625 MAPK pathway in resistant HR+ MBC,^{24,25} and MAPK pathway inhibition was
626 able to overcome this resistance. *RAS* mutations also activate the MAPK
627 pathway. The fact that multiple mechanisms of resistance to CDK4/6i activate the
628 MAPK pathway suggests that this may be an important node of resistance in
629 HR+ MBC – and that combining endocrine therapy and CDK4/6i with agents that
630 target MAPK such as MEK inhibitors, ERK inhibitors, and/or SHP2 inhibitors,
631 may be a unifying strategy to overcome or prevent resistance resulting from
632 multiple genetic aberrations. Similarly, both RB loss and AURKA amplification
633 are targetable with AURKA inhibitors. Taken together, it may be possible to
634 address all seven of these mechanisms (which account for at least 80% of the
635 resistant biopsies in this study) by targeting four nodes/pathways: AURKA,
636 MAPK, AKT/MTOR, and CCNE/CDK2 (Figure 6B).

637

638 We have identified multiple novel effectors of resistance to CDK4/6i in HR+
639 breast cancer, providing rationale to guide the development of a wide range of
640 precision-based clinical trials, in which patients with specific genomic or

641 molecular alterations are treated with novel therapeutic combinations designed to
642 circumvent or overcome resistance.

643 **Methods**

644 **Patients and Tumor Samples**

645 Prior to any study procedures, all patients provided written informed consent for
646 research biopsies and whole exome sequencing of tumor and normal DNA, as
647 approved by the Dana-Farber/Harvard Cancer Center Institutional Review Board
648 (DF/HCC Protocol 05-246). Metastatic core biopsies were obtained from patients
649 and samples were immediately snap frozen in OCT and stored in -80°C. Archival
650 FFPE blocks of primary tumor samples were also obtained. A blood sample was
651 obtained during the course of treatment, and whole blood was stored at -80°C
652 until DNA extraction from peripheral blood mononuclear cells (for germline DNA)
653 was performed. In a few instances, cell free DNA was obtained from plasma for
654 circulating tumor DNA analysis, as previously described.⁴⁹

655

656 **Clinical Annotation and Biopsy Phenotypes**

657 Patient charts were reviewed to determine the sequence of treatments received
658 in the neoadjuvant, adjuvant, and metastatic setting as well as the temporal
659 relationship between available biopsy samples and CDK4/6i exposure.
660 Radiographic parameters were assigned via review of the imaging study
661 interpretations available in the patient record during the CDK4/6i treatment
662 course – tumors were defined as “responding” if any degree of tumor shrinkage
663 was reported by the evaluating radiologist, “stable” if there was felt to be no
664 meaningful change, “progressing” if lesions were increasing in size, or “mixed” if
665 comment was made denoting simultaneous shrinkage and growth in discordant

666 lesions. Tumors with a mixed response were excluded from analysis as a reliable
667 phenotype could not be assigned. The “best radiographic response” (BRR) was
668 then assigned as either “response” (R), “stable disease” (S), or “progression” (P)
669 based upon the best radiographic parameter noted during the CDK4/6i treatment
670 course.

671

672 Sensitive biopsies were defined as baseline samples obtained within 120 days
673 prior to, or up to a maximum of 31 days after, CDK4/6i treatment initiation in a
674 patient with subsequent clinical benefit (radiographic response or stable disease
675 >6 months). Biopsies reflecting acquired resistance were obtained from patients
676 who had experienced clinical benefit with CDK4/6i and had an available biopsy
677 specimen either within 31 days of progression or at any time thereafter. Biopsies
678 reflecting intrinsic resistance were obtained within 120 days prior to CDK4/6i
679 initiation in patients without evidence of clinical benefit (defined as progression
680 on the first interval restaging study or stable disease <6 months).

681 **Whole Exome Sequencing**

682 DNA was extracted from primary tumors, metastatic tumors, and peripheral blood
683 mononuclear cells (for germline DNA) from all patients and whole exome
684 sequencing was performed, as detailed below. In several instances, cell free
685 DNA was obtained from plasma for circulating tumor DNA analysis, as previously
686 described.⁴⁹

687

688 **DNA extraction:** DNA extraction was performed as previously described.⁵⁰ For
689 whole blood, DNA is extracted using magnetic bead-based chemistry in
690 conjunction with the Chemagic MSM I instrument manufactured by Perkin Elmer.
691 Following red blood cell lysis, magnetic beads bind to the DNA and are removed
692 from solution using electromagnetized rods. Several wash steps follow to
693 eliminate cell debris and protein residue from DNA bound to the magnetic beads.
694 DNA is then eluted in TE buffer. For frozen tumor tissue, DNA and RNA are
695 extracted simultaneously from a single frozen tissue or cell pellet sample using
696 the AllPrep DNA/RNA kit (Qiagen). For FFPE tumor tissues, DNA and RNA are
697 extracted simultaneously using Qiagen's AllPrep DNA/RNA FFPE kit. All DNA is
698 quantified using Picogreen

699

700 **Library Construction:** DNA libraries for massively parallel sequencing were
701 generated as previously described⁵⁰ with the following modifications: the initial
702 genomic DNA input into the shearing step was reduced from 3 μ g to 10-100ng in
703 50 μ L of solution. For adapter ligation, Illumina paired-end adapters were
704 replaced with palindromic forked adapters (purchased from Integrated DNA
705 Technologies) with unique dual indexed 8 base index molecular barcode
706 sequences included in the adapter sequence to facilitate downstream pooling.
707 With the exception of the palindromic forked adapters, all reagents used for end
708 repair, A-base addition, adapter ligation, and library enrichment PCR were
709 purchased from KAPA Biosciences in 96-reaction kits. In addition, during the
710 post-enrichment solid phase reversible immobilization (SPRI) bead cleanup,

711 elution volume was reduced to 30 μ L to maximize library concentration, and a
712 vortexing step was added to maximize the amount of template eluted.

713

714 ***Solution-phase hybrid selection:*** After library construction, hybridization and
715 capture were performed using the relevant components of Illumina's Rapid
716 Capture Exome Kit and following the manufacturer's suggested protocol, with the
717 following exceptions: first, all libraries within a library construction plate were
718 pooled prior to hybridization. Second, the Midi plate from Illumina's Rapid
719 Capture Exome kit was replaced with a skirted PCR plate to facilitate automation.
720 All hybridization and capture steps were automated on the Agilent Bravo liquid
721 handling system.

722

723 ***Preparation of libraries for cluster amplification and sequencing:*** After post-
724 capture enrichment, library pools were then quantified using quantitative PCR
725 (KAPA Biosystems) with probes specific to the ends of the adapters; this assay
726 was automated using Agilent's Bravo liquid handling platform. Based on qPCR
727 quantification, libraries were normalized and denatured using 0.1 N NaOH on the
728 Hamilton Starlet.

729

730 ***Cluster amplification and sequencing:*** Cluster amplification of denatured
731 templates was performed according to the manufacturer's protocol (Illumina)
732 using HiSeq 2500 Rapid Run v1/v2, HiSeq 2500 High Output v4 or HiSeq 4000
733 v1 cluster chemistry and HiSeq 2500 (Rapid or High Output) or HiSeq 4000

734 flowcells. Flowcells were sequenced on HiSeq 2500 using v1 (Rapid Run
735 flowcells) or v4 (High Output flowcells) Sequencing-by-Synthesis chemistry or v1
736 Sequencing-by-Synthesis chemistry for HiSeq 4000 flowcells. The flowcells were
737 then analyzed using RTA v.1.18.64 or later. Each pool of whole exome libraries
738 was run on paired 76np runs, with a two 8 base index sequencing reads to
739 identify molecular indices, across the number of lanes needed to meet coverage
740 for all libraries in the pool.

741

742 ***Sequence data processing:*** Exome sequence data processing was performed
743 using established analytical pipelines at the Broad Institute. A BAM file was
744 produced with the Picard pipeline (see URLs) which aligns the tumor and normal
745 sequences to the hg19 human genome build using Illumina sequencing reads.
746 The BAM was uploaded into the Firehose pipeline (see URLs), which manages
747 input and output files to be executed by GenePattern⁵¹.

748

749 ***Sequencing quality control:*** Quality control modules within Firehose were
750 applied to all sequencing data for comparison of the origin for tumor and normal
751 genotypes and to assess fingerprinting concordance. Cross-contamination of
752 samples was estimated using ContEst.⁵²

753

754 **Somatic Alteration Assessment**

755 MuTect⁵³ was applied to identify somatic single-nucleotide variants. Indelocator
756 (see URLs), Strelka⁵⁴, and MuTect2 (see URLs) were applied to identify small

757 insertions or deletions. A voting scheme with inferred indels requiring at least 2
758 out of 3 algorithms.

759

760 Artifacts introduced by DNA oxidation (so called OxoG) during sequencing were
761 computationally removed using a filter-based method.⁵⁵ In the analysis of primary
762 tumors that are formalin-fixed, paraffin-embedded samples [FFPE] we further
763 applied a filter to remove FFPE-related artifacts.⁵⁶

764

765 Reads around mutated sites were realigned with Novoalign (see URLs) to filter
766 out false positive that are due to regions of low reliability in the reads alignment.
767 At the last step, we filtered mutations that are present in a comprehensive WES
768 panel of 8,334 normal samples (using the Agilent technology for WES capture)
769 aiming to filter either germline sites or recurrent artifactual sites. We further used
770 a smaller WES panel of normal 355 normal samples that are based on Illumina
771 technology for WES capture, and another panel of 140 normals sequenced within
772 our cohort²⁷ to further capture possible batch-specific artifacts. Annotation of
773 identified variants was done using Oncotator.⁵⁷

774

775 **Copy Number and Copy Ratio Analysis**

776 To infer somatic copy number from WES, we used ReCapSeg (see URLs),
777 calculating proportional coverage for each target region (i.e., reads in the
778 target/total reads) followed by segment normalization using the median coverage

779 in a panel of normal samples. The resulting copy ratios were segmented using
780 the circular binary segmentation algorithm.⁵⁸

781

782 To infer allele-specific copy ratios, we mapped all germline heterozygous sites in
783 the germline normal sample using GATK Haplotype Caller⁵⁹ and then evaluated
784 the read counts at the germline heterozygous sites in order to assess the copy
785 profile of each homologous chromosome. The allele-specific copy profiles were
786 segmented to produce allele specific copy ratios.

787

788 **Gene deletions and Bi-allelic inactivation**

789 For the inference of gene deletions and inactivations, as we aim to infer bi-allelic
790 inactivations (BiDel or “HOMDEL”), we take into account various mutational
791 events that may result in inactivation of both alleles. These mutational events
792 include: (1) loss of heterozygosity (LOH), (2) SNV (while excluding the following
793 variant classifications: “Silent”, “Intron”, “IGR”, “5’UTR”, “3’UTR”, “5’Flank”,
794 “3’Flank”), (3) short indels, (4) long deletions and gene rearrangements inferred
795 by SvABA,⁶⁰ and (5) potentially pathogenic germline events in cancer genes (see
796 description below).

797 Potentially pathogenic germline events: aiming to retain a subset of potentially
798 pathogenic germline events there are several features which are accounted for
799 including (1) ClinVar significant annotation among the following: Pathogenic.
800 Likely pathogenic, Conflicting interpretations of pathogenicity, risk factor or (2)
801 Variant Classification among the following: Splice_Site, Frame_Shift_Del,

802 Frame_Shift_Ins, Nonsense_Mutation. In addition (3) Genome Aggregation
803 Database (gnomAD)⁶¹ less than 0.05 (indicating it is a rare variant)

804

805 **Cancer Cell Fraction and Evolutionary Analysis**

806 ***Analysis using ABSOLUTE:*** To properly compare SNVs and indels in paired
807 metastatic and primary samples, we considered the union of all mutations called
808 in either of the two samples. We evaluated the reference and alternate reads in
809 each patient's primary and metastatic tumors, including mutations that were not
810 initially called in one of the samples. These mutations in matched samples were
811 used as input for ABSOLUTE.⁶² The ABSOLUTE algorithm uses mutation-
812 specific variant allele fractions (VAF) together with the computed purity, ploidy,
813 and segment-specific allelic copy-ratio to compute cancer cell fractions (CCFs).

814

815 **Clonal structure and phylogenetic reconstruction of tumor evolution**

816 The clonal structure observed in individuals with more than a single tumor
817 sample was inferred with PyClone,⁶³ using the Beta Binomial model and the copy
818 number of each mutation inferred by ABSOLUTE with the parental copy number
819 parameter.

820 Subsequently, the inferred clonal structure was used to trace the evolutionary
821 history of the clones (phylogenetic tree) using the ClonEvol,⁶⁴ retaining only clones
822 with at least four mutations and estimated cancer cellular fraction (cellular
823 prevalence) higher than 1%.

824

825 **Evolutionary analysis of copy-number variation**

826 ***Corrected quantification of copy number:*** gene amplifications are based on
827 the purity corrected measure for the segment containing that gene, based on
828 ABSOLUTE (rescaled_total_cn).⁶² To better measure segment-specific copy-
829 number, we subtracted the genome ploidy for each sample to compute copy
830 number above ploidy (CNAP). CNAP of at least 3 are considered as
831 amplifications (“AMP”), CNAP above 1.5, but below 3 are considered low
832 amplification (“GAIN”), and are not depicted in our mutational landscape (Figure
833 1). CNAP of at least 6 are considered high amplifications (“HighAMP”), and
834 CNAP of at least 9 and no more than 100 genes⁶⁵ is considered very high focal
835 amplification (“FocalAMP”).

836 The evolutionary classification of amplifications accounts for the magnitude of the
837 observed copy-number difference between the pre-treatment and the post-
838 treatment samples. If the difference between the CNAP of the post-treatment and
839 the CNAP of the pre-treatment is smaller than 50%, the amplification is defined
840 as “Shared”. If the CNAP of the post-treatment is larger than the CNAP by more
841 than 50% and the lower pre-treatment CNAP is not at “FocalAMP” level, the
842 evolutionary classification is “Acquired”. If CNAP of the post-treatment is smaller
843 by at least 50%, comparing to the pre-treatment sample and the lower post-
844 treatment CNAP is not at “FocalAMP” level, the evolutionary classification is
845 “Loss”. Otherwise, the evolutionary classification of amplifications is defined as
846 “Indeterminate”.

847

848 **Cell Culture**

849 HR+/HER2- human breast cancer cell lines T47D (HT-133) and MCF7 (HTB-22)
850 were obtained from American Type Culture Collection (ATCC). T47D and MCF7
851 cells were cultured in RPMI 1640 medium (no phenol red; Gibco, 11835-030) and
852 MEMα (nucleosides, no phenol red; Gibco, 41061029) respectively, both
853 supplemented with 10% fetal bovine serum (Gemini bio-products, 100-106) and
854 1% penicillin-streptomycin-glutamine. HEK 293T/17 (CRL-11268) were obtained
855 from ATCC and cultured in DMEM (high glucose, pyruvate; Gibco, 11995065),
856 supplemented with 10% fetal bovine serum (Gemini bio-products, 100-106) and
857 1% penicillin-streptomycin-glutamine (Gibco, 10378016).

858

859 **Candidate driver plasmid and cell line production**

860 AKT1 (BRDN0000464992), KRASG12D (BRDN0000553331), AURKA
861 (TRCN0000492002), CCNE2 (ccsbBroadEn_11340), and GFP bacterial streaks
862 were obtained from the Genetic Perturbation Platform, Broad Institute, MA. RB1
863 and CRISPR non-targeting guide cells were obtained as a gift Flora Luo and the
864 Garraway laboratory. The CCNE2 construct was cloned into a pLX307 vector
865 using the LR reaction kit (Life Technologies, 11791019). All construct plasmids
866 were prepared using the Plasmid Plus Midi Kit (Qiagen, 12943). To generate
867 lentivirus for each construct, 293T cells were transfected with Opti-MEM (Gibco,
868 31985-062), FuGENE HD (Promega, E2311), VSV-G envelope plasmid, and
869 □8.91 packaging plasmid. After 72h of incubation, supernatant was filtered
870 through a 0.45 µL filter (Corning, 431225) and lentivirus presence was tested

871 using Lenti-X GoStix (TakaraBio, 631244). 500 μ L – 1mL of virus was added to a
872 60-mm dish containing T47D (or MCF7) cells and medium with 4 μ g/mL of
873 polybrene (Millipore Sigma, TR-1003-G). After overnight incubation, cells were
874 moved to a 100-mm dish and again incubated overnight. The medium was
875 replaced and 0.5 μ g/mL of puromycin (Gibco, A1113803) were added to
876 KRASG12D, AURKA, CCNE2, RB1 and CRISPR constructs, and 6-10 μ g/mL of
877 blasticidin (Gibco, A1113903) were added to GFP and AKT1 constructs. Plates
878 were compared to uninfected control plates, and after 2 days of selection, were
879 plated for drug sensitivity assay and harvested for western blotting as described
880 below.

881

882 **Kill Curves/Drug Sensitivity Assay**

883 Cells were plated at a density of 1000 cells/well in RPMI and 1500 cells/well in
884 MEM α , for T47D and MCF7, respectively, in 96 well plates (PerkinElmer,
885 6005181). The experiments were plated in triplicate, for ten doses of the drug of
886 interest. Palbociclib doses ranging from 1 nM to 10 μ M were prepared from a 10
887 mM stock solution in molecular biology grade water (Corning, 46-000-CI);
888 abemaciclib doses ranging from 1 nM to 10 μ M were prepared from a 10 mM
889 stock solution in molecular biology grade water (Corning, 46-000-CI); fulvestrant
890 doses ranging from 0.01 nM to 1 μ M were prepared from a 20 mM stock solution
891 in DMSO (Sigma-Aldrich, D2650). The next day, cells were treated with the
892 range of doses of the drug of interest. Cells were re-treated three days later.
893 After treatment has been applied for eight days, the 96-well plates were brought

894 out of the incubator and allowed to equilibrate to room temperature. The medium
895 was replaced with 50 μ L of fresh medium per well. 50 μ L of CellTiter-Glo 2.0
896 (Promega, G9241) was added to each well, the plate was shaken at 200 rpm for
897 2 min, and then allowed to equilibrate at room temperature for fifteen minutes as
898 per the CellTiter-Glo 2.0 Assay Technical Manual. Average background
899 luminesce reading was calculated from plate wells containing only medium, and
900 was subtracted from all values. The values were then averaged for each triplicate
901 and standard deviations were calculated. The data were normalized to the no-
902 drug, vehicle control for each construct. The calculated averages and standard
903 deviations were visualized on GraphPad Prism 7 using the log(inhibitor) vs.
904 response (three parameters) preset protocol.

905

906 **Chemicals and antibodies**

907 Chemicals utilized included palbociclib (Selleck Chemicals, S1116), abemaciclib
908 (ApexBio, A1794), and fulvestrant (Sigma-Aldrich, I4409). Primary antibodies
909 utilized included antibodies against β -Actin (Santa Cruz, sc-47778), Rb (Cell
910 Signaling Technology, clone 4H1, 9309), Akt (CST, 9272), Ras (CST, clone
911 D2C1, 8955), Aurora A (CST, clone D3E4Q, 14475), and Cyclin E2 (CST, 4132),
912 in addition to the secondary antibodies goat anti-rabbit (Invitrogen, 32260) and
913 goat anti-mouse (Invitrogen, A16090).

914

915 **Western blotting**

916 A near-confluent T75 (~7x10⁶ cells) was spun down and the pellet kept at -20C.
917 The pellet was then lysed in 1mL of lysis buffer consisting of RIPA buffer (Sigma-
918 Aldrich, R0278), dithiothreitol (DTT, Invitrogen, 15508013), phenylmethane
919 sulfonyl fluoride (PMSF, Sigma-Aldrich, P7626), and PhosStop (Sigma-Aldrich,
920 4906837001). Lysate was rotated at 15 r.p.m for 15 minutes at 4°C, then
921 centrifuged at 14,000g for 15 minutes at 4°C, preserving the supernatant. Protein
922 concentration was quantified via bicinchoninic acid assay (Pierce BCA Protein
923 Assay Kit, Thermo Fisher Scientific, 23225) and Tecan i-control software pre-set
924 BCA program. Samples were prepared using 40µg of protein, Bolt LDS Sample
925 Buffer (Invitrogen, B0007), and DTT and heated to 95°C for 5 min. The samples
926 were run on a Bolt 4-12% Bis-Tris Plus Gel (Invitrogen, NW04120BOX) in 1X
927 Bolt MOPS SDS Running Buffer (Invitrogen, B000102) for 1hr at 130V. Protein
928 was transferred to nitrocellulose membranes via the Trans-Blot Turbo Transfer
929 System (Bio-Rad, 1704150) following the turbo mini preset protocol (1.3A 25V
930 7Min) two times. Membranes were blocked in 5% milk in Tris-buffered saline
931 (Bio-Rad, 1706435) with 0.1% Tween-20 (Sigma-Aldrich, P9416) for one hour at
932 room temperature. Membranes were incubated overnight at 4°C with primary
933 antibodies that were diluted 1:1000 (with the exception of Rb, which was diluted
934 1:500) in 5% milk in TBS-T. After incubation, membranes were washed 3 times
935 for 10min with 1X TBS-T and incubated with secondary antibody diluted 1:2000
936 in 5% milk in TBS-T for 1h at room temperature. Membranes were then washed
937 3 times for 10min with 1X TBS-T. After washing, membranes were treated with

938 Pierce ECL Plus Western Blotting Substrate (Thermo Fisher Scientific, 32132) for
939 5 minutes and exposed to autoradiography film (Denville, 1159M38).

940

941 For resistant/derivative cell lines: cells were washed with PBS and lysed in lysis
942 buffer (1% triton X-100, 25mM Tris pH 7.5, 150mM NaCl, 1mM EDTA, Halt
943 Protease/phosphatase inhibitor cocktail), and protein concentration was
944 assessed by BCA protein assay (Pierce 23225). Equal amounts of protein were
945 electrophoresed on 4-20% BioRad Tris Glycine Gels (BioRad 5671094)
946 transferred to nitrocellulose (BioRad 1704159) and probed with primary
947 antibodies. Antibodies were purchased from Cell Signaling Technology for Rb
948 Total (9307), pRb S780 (3590), pRb S807/811 (8516), CCNE2 (4132), Akt S473
949 (4051), S6 total (2317), S6 S240/244 (4838), ERK total (3042), pERK T202/Y204
950 (4370, 4376) and R&D Systems AurA (AF3295). Digiwest® protein profiling of
951 MDA-MB-361-AR was also conducted with NMI TT.

952

953

954 **Resistant cell line generation**

955 The methods for generating resistant cell lines were described previously.³⁴
956 Briefly, MDA-MB-361, T47D and MCF-7 ER+ breast cancer cell lines were used
957 to derive variants with acquired resistance to abemaciclib or palbociclib. T47D
958 (HTB-133), MCF-7 (HTB-22) and MDA-MB-361 (HTB-27) were purchased from
959 The American Type Culture Collection (ATCC). Cell lines were cultured in RPMI-
960 1640 medium (Gibco 22400-089) + 10% FBS (Hyclone SH30071.03), Eagles

961 Essential Medium (Gibco 11090-081) + 10% FBS and Liebovitz L-15 Medium
962 (Gibco 11215-064) + 20% FBS, respectively. Resistant cell lines were generated
963 by chronic treatment with either abemaciclib or palbociclib alone or in
964 combination with fulvestrant. Cell cultures were initiated in low doses of
965 compound approximating the IC50 until cells grew to 80% confluence. Cells were
966 then passaged and treated with incrementally higher doses. This process was
967 repeated several times until cells were able to grow in the presence of drugs at
968 clinically meaningful concentrations. Once resistant cell lines were established,
969 the stability of resistance was assessed with a 21 day dosing holiday. Resistance
970 remained stable in all cell lines except for T47D-AR and T47D-PR which became
971 almost completely resensitized to the CDK4/6i after the 21 day drug-free period.
972 All resistant derivatives resistant were found to be cross resistant to the CDk4/6i
973 that was not used in the selection step. Short tandem repeat (STR) analysis was
974 performed to verify the authenticity of the cell lines.

975

976 **Proliferation Assays**

977 Cells were plated onto poly-D-lycine plates (Corning 354640) and treated in
978 replicate with a dose curve of compounds of interest. Cells were allowed to grow
979 for two doubling times and proliferation was measured by CellTiter-Glo®
980 (Promega G7571) or CyQuant (Invitrogen C3511) per manufacturer's protocol.
981 Data analysis was carried out using Prism software.

982

983 **LY3295668 Phase 1/2 Clinical Trial**

984 The patient vignette provided in this manuscript was shared from an ongoing
985 phase 1/2 study. Please see protocol NCT03092934 at www.clinicaltrials.gov for
986 details related to the study location, eligibility, and compound. This is an open-
987 label, multicenter study of patients with locally advanced or metastatic solid
988 tumors and disease progression after 1-□4 prior treatment regimens. The phase
989 1 portion of the protocol is designed to evaluate the primary objective of
990 determining the maximum tolerated dose (MTD); secondary objectives included
991 evaluation of tolerability and overall safety profile of LY3295668. The primary
992 objective of the phase 2 study portion is to evaluate the objective response rate
993 of tumors after treatment with LY3295668. Patients in the phase 2 study were
994 required to have estrogen receptor and/or progesterone receptor positive, human
995 epidermal growth factor receptor 2 (HER2) negative, breast cancer with prior
996 exposure to and progression on on a hormone therapy and a CDK4/6 inhibitor.

997

998 **Acknowledgements**

999 We thank Laura Dellostritto, Lori Marini, Nelly Oliver, Shreevidya Periyasamy,
1000 Janet Files, Sara Hoffman, and Colin Mackichan for assistance with patient
1001 sample collection and annotation. We are grateful to all the patients who
1002 volunteered for our tumor biopsy protocol and generously provided the tissue
1003 analyzed in this study.

1004

1005 **Grant support**

1006 This work was supported by the Department of Defense W81XWH-13-1-0032
1007 (NW), AACR Landon Foundation 13-60-27-WAGL (NW), NCI Breast Cancer
1008 SPORE at DF/HCC #P50CA168504 (NW, NUL and EPW), Susan G. Komen
1009 CCR15333343 (NW), The V Foundation (NW), The Breast Cancer Alliance (NW),
1010 The Cancer Couch Foundation (NW), Twisted Pink (NW), Hope Scarves (NW),
1011 Breast Cancer Research Foundation (NUL and EPW), ACT NOW (to Dana-
1012 Farber Cancer Institute Breast Oncology Program), Fashion Footwear
1013 Association of New York (to Dana-Farber Cancer Institute Breast Oncology
1014 Program), Friends of Dana-Farber Cancer Institute (to NUL), National
1015 Comprehensive Cancer Network/Pfizer Independent Grant for Learning &
1016 Change (to NUL), the Dana-Farber Cancer Institute T32 (to SAW), Wong Family
1017 Translational Research Award (to SAW), and the Conquer Cancer
1018 Foundation/Twisted Pink/American Society of Clinical Oncology Young
1019 Investigator Award (to SAW).
1020

1021 **Figure Legends**

1022 **Figure 1. The genomic landscape of CDK4/6i resistance is heterogeneous,
1023 with multiple potential driver events.**

1024 (a) Biopsy phenotypes were assigned as *sensitive*, *acquired resistance*, or
1025 *intrinsic resistance* based upon timing of the biopsy relative to CDK4/6i exposure
1026 (d - days), best radiographic response (BRR), and duration of treatment. Patients
1027 were categorized as experiencing clinical benefit on CDK4/6i if interval restaging
1028 demonstrated a response or disease stability for at least six months. (b)
1029 Mutational matrix (CoMut) depicting the genomic landscape of the CDK4/6i
1030 cohort (n = 59 biopsies, 58 patients). Copy number alterations and mutational
1031 events in select genes of interest are shown. Clinical parameters (shown at the
1032 top) include receptor status, anti-estrogen agent, CDK4/6 inhibitor, best
1033 radiographic response (P – progression, R – response, S – stable), biopsy
1034 phenotype (S – sensitive, IR – intrinsic resistance, AR – acquired resistance),
1035 treatment duration (days), biopsy timing relative to treatment initiation (days),
1036 time since metastatic diagnosis (days), and number of lines of prior treatment. (c)
1037 Phenotype distribution plot demonstrating a higher frequency of copy number
1038 amplifications in Aurora Kinase A (AURKA) among resistant biopsies (AR + IR,
1039 left) compared to sensitive biopsies (right, 0.0081, Welch test). (d) Bar plot
1040 visualization of mutational (M) and/or copy number alterations (A – amplification,
1041 LA – low amplification) in select genes. The proportional enrichment (fraction of
1042 samples demonstrating alteration) in sensitive biopsies (left, blue) and resistant
1043 biopsies (AR + IR, right, red) is included.

1044

1045 **Figure 2. Acquired resistance to CDK4/6i in patients with pre-treatment and**
1046 **post-progression biopsies demonstrates convergent evolution of biallelic**
1047 **RB1 disruption and evolved AKT1 activation.**

1048 Phylogenetic analysis depicting the evolutionary history for seven patients with
1049 acquired alterations, with clonal evolutionary dynamics demonstrating: (a)
1050 acquired polyclonal ESR1 mutations after aromatase inhibition, followed by
1051 convergent evolution of RB1 inactivation, with different RB1-inactivating
1052 mutations acquired in two parallel sibling clones; (b) Acquired AKT1
1053 amplification; (c) No notable candidate for acquired mechanism of resistance
1054 (MOR); (d) Acquired AKT1 (W80R) mutation; (e) No notable candidate for
1055 acquired MOR; (f) Acquired inactivation of DNA Mismatch Repair Protein
1056 (MLH3); and (g) Acquired activating ESR1 mutation (Y537S) and amplification in
1057 AKT3.

1058

1059 **Figure 3. Clinical vignettes for candidate resistance drivers in**
1060 **representative patients (RB1, AKT1, RAS, and CCNE2).**

1061 Clinical vignettes including treatment sequence, timing of metastatic progression,
1062 and available biopsies with key genomic findings are provided for the following -
1063 (a) four patients with biallelic alterations in RB1, including a patient with multiple
1064 biopsies and convergent evolution toward RB1 disruption (top, phylogenetic
1065 analysis for this patient is provided in Figure 2A). (b) Three patients with acquired
1066 alterations in AKT1 following progression on CDK4/6i. In the first (top), a new

1067 mutation in AKT1 W80R was identified. In the second (middle), a baseline
1068 alteration (AKT1 L52H) was identified at the time of diagnosis; at the time of
1069 progression on CDK4/6i, two biopsies were obtained – both demonstrating the
1070 baseline AKT1 L52H mutation, one also demonstrating an acquired amplification
1071 of the wild-type AKT1 protein (phylogenetic analyses for these patients are
1072 provided in Figure 2B and D). (c) Three patients with resistance to CDK4/6i and
1073 RAS-family alterations (including two instances of KRAS G12D and one instance
1074 of HRAS mutation). (d) Three patients with intrinsic resistance to CDK4/6i and
1075 amplification events in CCNE2.

1076

1077 **Figure 4. Candidate genomic alterations provoke CDK4/6i resistance *in***
1078 ***vitro*.**

1079 (a) T47D cells were modified via CRISPR-mediated downregulation (RB1) or
1080 lentiviral overexpression (AKT1, KRAS G12D, AURKA, CCNE2) to interrogate
1081 potential resistance mediators identified in patient biopsy samples. Western
1082 blotting with the indicated antibodies is included. (b-f) Modified T47D cells were
1083 exposed to escalating doses of CDK4/6i (palbociclib – left, abemaciclib – right)
1084 and viability was estimated via cell-titer-glo (CTG) assay. Control (CRISPR non-
1085 targeting guide or GFP) cells are plotted along with the resistance driver of
1086 interest (RB1 – b, AKT1 – c, KRAS G12D – d, AURKA – e, CCNE2 – f). Parental
1087 and variant cell lines are normalized to vehicle control and viability is plotted as a
1088 function of increasing CDK4/6i (graphed as triplicate average +/- standard
1089 deviation). All variants provoke CDK4/6i resistance (to both palbociclib and

1090 abemaciclib) *in vitro* in T47D cells. Corresponding IC50 values are included in
1091 Supplemental Table 7.

1092

1093 **Figure 5. Candidate mutations emerge in cell lines cultured under CDK4/6i**
1094 **selective pressure and define new therapeutic dependencies *in vitro*.**

1095 (a) Breast cancer cell lines (T47D, MCF7, MDA-MB-361) were cultured long-term
1096 to resistance in the presence of CDK4/6i (palbociclib, abemaciclib). The resulting
1097 cell lines which emerged were subjected to western blotting for putative
1098 mediators of drug resistance (RB1, AKT1, KRAS/ERK, AURKA, and CCNE2). (b-
1099 c) T47D cells cultured to resistance in the presence of abemaciclib demonstrated
1100 low levels of RB1 expression (T47D-AR1) and increased sensitivity to the
1101 AURKA inhibitor LY3295668. MDA-MB-361 cells cultured to resistance in the
1102 presence of abemaciclib demonstrated high levels of ERK activation (361-AR1)
1103 and increased sensitivity to the ERK inhibitor LY3214996. MDA-MB-361 cells
1104 cultured to resistance in the presence of palbociclib demonstrated high levels of
1105 AURKA (361-PR1) and increased sensitivity to the AURKA inhibitor LY3295668.
1106 MCF7 cells cultures to resistance in the presence of palbociclib demonstrated
1107 increased levels of CCNE2 (MCF7-PR1) and increased sensitivity to the CHEK1
1108 inhibitor prexasertib.

1109

1110 **Figure 6. A novel aurora kinase A inhibitor demonstrates therapeutic**
1111 **efficacy in a patient with metastatic HR+ breast cancer after progression on**
1112 **CDK4/6i.**

1113 (a) A patient with locally advanced HR+/HER2- breast cancer developed
1114 metastatic recurrence on adjuvant tamoxifen. She received CDK4/6i and
1115 letrozole in the first line setting with prolonged clinical benefit (>3 years). At
1116 progression, she was placed on trial with the AURKA inhibitor LY3295668; she
1117 subsequently experienced prolonged disease control ~11 months. Baseline
1118 staging studies following progression on CDK4/6i in the patient described are
1119 included (top); she had osseous metastatic disease and visceral disease limited
1120 to the foci noted in the liver. Two interval restaging studies (top) demonstrate
1121 disease stability/mild response. Liver biopsy obtained at the time of progression
1122 on CDK4/6i and prior to LY3295668 demonstrated high Ki67 and high RB1
1123 protein expression via immunohistochemistry (IHC, 10x) (bottom). (b) Schematic
1124 diagram demonstrating the potential utility of next-generation sequencing
1125 following progression on CDK4/6i; actionable alterations in RB1, ERBB2,
1126 FGFR2, AKT1, RAS, AURKA, and CCNE2 could dictate informed selection of
1127 targeted therapies as indicated.

1128

1129 **Supplementary Figure Legends**

1130

1131 **Supplemental Figure 1. Subgroup genomic analysis of the CDK4/6i cohort**
1132 **based upon anti-estrogen exposure.**

1133 Heatmaps demonstrating key genomic events (both copy number alteration and
1134 mutation) in a subset of genes for (a) patients with exposure to CDK4/6i and
1135 aromatase inhibitor (AI) and for (b) patients with exposure to CDK4/6i and
1136 fulvestrant. The gene set and clinical parameters are identical to those provided
1137 in Figure 1B.

1138

1139 **Supplemental Figure 2. Higher AURKA expression observed even in low-**
1140 **amplification tumors in TCGA**

1141 Breast tumor from the TCGA dataset were stratified based on the genomic
1142 AURKA copy number (low amplification – left, no amplification – right; high
1143 amplification excluded) and plotted against AURKA RNA expression. Higher
1144 AURKA RNA expression was observed in low AURKA-amplification compared to
1145 non-amplified tumors in these TCGA samples.

1146

1147

1148 **Supplemental Figure 3. Candidate resistance mutations in representative**
1149 **patients – key counterexamples.**

1150 Biopsies demonstrating CDK4/6i sensitivity despite the presence of putative
1151 resistance drivers were identified and clinical vignettes were generated. (a) A

1152 patient with bone-only metastatic progression was placed on first-line CDK4/6i
1153 and letrozole. A canonical AKT1 E17K alteration was identified at the time of
1154 metastatic progression. This patient has had stable osseous metastatic disease
1155 on interval repeat imaging and remained on treatment at the time of data cutoff.
1156 (b) A patient with de novo metastatic HR+/HER2- breast cancer was treated with
1157 tamoxifen and subsequently received palbociclib and letrozole. Prior to CDK4/6i
1158 exposure, which lasted for a duration exceeding one year, a baseline low-level
1159 amplification in CCNE2 was identified. (c) A patient was diagnosed with localized
1160 HR-/HER2+ breast cancer and treated with chemotherapy. Late metastatic
1161 relapse occurred with a new contralateral tumor, now HR+/HER2-. Following
1162 progression on tamoxifen, and prior to treatment with CDK4/6i and letrozole, an
1163 ERBB2 mutation was identified. Despite the presence of this alteration, the
1164 patient has had a durable ongoing response to CDK4/6i-based treatment.

1165

1166 **Supplemental Figure 4. Candidate alterations provoke CDK4/6i resistance**
1167 ***in vitro* (MCF7).**

1168 (a) MCF7 cells were modified via CRISPR-mediated downregulation (RB1) or
1169 lentiviral overexpression (AKT1, KRAS G12D, AURKA, CCNE2) to interrogate
1170 potential resistance mediators identified in patient biopsy samples. Western
1171 blotting with the indicated antibodies is included. (b-f) Modified MCF7 cells were
1172 exposed to escalating doses of CDK4/6i (palbociclib – left, abemaciclib – right)
1173 and viability was estimated via cell-titer-glo (CTG) assay. Control (CRISPR non-
1174 targeting guide, GFP) cells are plotted along with the resistance driver of interest

1175 (RB1 – b, AKT1 – c, KRAS G12D – d, AURKA – e, CCNE2 – f). Parental and
1176 variant cell lines are normalized to vehicle control and viability is plotted as a
1177 function of increasing CDK4/6i (graphed as triplicate average +/- standard
1178 deviation). RB1, AKT1, and CCNE2 provoke CDK4/6i resistance (to both
1179 palbociclib and abemaciclib) *in vitro* in MCF7 cells. Corresponding IC50 values
1180 are included in Supplemental Table 7.

1181

1182 **Supplemental Figure 5. Candidate alterations provoke variable anti-**
1183 **estrogen resistance *in vitro*.**

1184 Cell lines modified to reflect potential resistance drivers (per Figure 4 and
1185 Supplemental Figure 6; T47D – left, MCF7 - right) were exposed to escalating
1186 doses of fulvestrant (a – e). Drug response was assessed via cell-titer-glo (CTG)
1187 assay. Control (CRISPR non-targeting guide, GFP) cells are plotted along with
1188 the resistance driver of interest (RB1 – a, AKT1 – b, KRAS G12D – c, AURKA –
1189 d, CCNE2 – e). Parental and variant cell lines are normalized to vehicle control
1190 and viability is plotted as a function of increasing CDK4/6i (graphed as triplicate
1191 average +/- standard deviation). AKT1 and CCNE2 provoke fulvestrant
1192 resistance *in vitro* in both T47D and MCF7 cells. RB1 provokes minimal
1193 fulvestrant resistance in both T47D and MCF7. KRAS G12D and AURKA
1194 provoke significant fulvestrant resistance in T47D; KRAS G12D provokes
1195 minimal resistance in MCF7, while AURKA does not convey any resistance in
1196 MCF7. Corresponding IC50 values are included in Supplemental Table 7.

1197

1198 **Supplemental Figure 6. MDA-MB-361-AR-1 demonstrates upregulation of**
1199 **RAS-ERK pathway effectors via proteomic analysis.**

1200 Digiwest proteomic analysis of MDA-MB-361-AR-1 cells versus parental MCF-7
1201 cells demonstrates increased activation of multiple RAS-pathway effectors
1202 including KRAS, MEK, and ERK. These results suggest that the upregulation in
1203 pERK noted via western blot analysis correlates with pathway activation in the
1204 derivative cells.

1205 **Supplementary Table Legends**

1206

1207 **Supplemental Table 1. Clinical samples included in landscape analysis**
1208 **(excel file, 1 tab)**

1209 Clinical information including treatment regimen, treatment duration (days), best
1210 radiographic response (BRR), and timing of the biopsy relative to treatment
1211 initiation/cessation (days). Biopsy sample information including receptor status,
1212 biopsy site, cancer-purity of sample and treatment-related information

1213

1214 **Supplemental Table 2. Clinical cohort characteristics (excel file, 1 tab)**

1215 Clinical parameters of interest are included at the patient level (n = 58).

1216

1217 **Supplemental Table 3. Exome and mutational information (excel file, 3 tabs)**

1218 Tab 1 – Exome-wide single nucleotide variants (SNVs) and Indels; Tab 2- Copy
1219 Number Variants (CNVs) at the segment level including Copy Number Above
1220 Ploidy (CNAP); Tab 3 - CNVs and Bi-Allelic inactivation at the single-gene level
1221 among oncogene and tumor suppressor gene candidates; Tab 4 – Genomic
1222 alterations among candidate mechanisms of resistance (MOR) among the
1223 resistance samples in our cohort. Candidate MOR genes include – RB1 with
1224 HOMDEL mutation type, AURKA - with Amplifications including GAIN) CCNE2
1225 AKT1, RAS (KRAS, NRAS, and HRAS), ERBB2, and FGFR (FGFR1, FGFR2,
1226 and FGF3) – with activating events – Amplifications and putative activating SNVs;

1227 Tab 5 – literature based list of known oncogenes (n=489) and tumor suppressor
1228 gene candidates (n=483).⁴⁵⁻⁴⁸

1229

1230 **Supplemental Table 4. Enrichment analysis of mutation in resistant vs.**
1231 **sensitive tumors (excel file, 1 tab)**

1232 Fisher's Exact test (single-side, for enrichment) comparing gene-specific the
1233 frequency of mutational events: HOMDEL==Bi-Allelic inactivation (among tumor
1234 suppressor candidates), IHC loss (for ER receptor), and gene activation by copy-
1235 number amplification – GAIN.up== CNAP>=1.5, AMP.up== CNAP>=3, or gene
1236 activation by either amplification or activating mutation – ACT==CNAP>=3 or
1237 Gain-of-function or recurring mutation, ACT.inc== same as ACT, but including
1238 non-recurring missense mutation (among oncogene candidates)

1239

1240 **Supplemental Table 5. Driver enrichment within patient populations (excel**
1241 **file, 1 tab)**

1242 Sensitive, intrinsic resistant, and acquired resistant biopsies harboring any of the
1243 8 potential driver alterations are quantified and graphed in figure 1D. Potential
1244 driver alterations include ER loss, amplification/mutation of ERBB2, FGFR2,
1245 CCNE2, AURKA, RAS, AKT1 and biallelic disruption of RB1.

1246

1247 **Supplemental Table 6. Evolutionary analysis and clonal fraction across 7**
1248 **patients with multiple biopsies spanning pre- and post-treatment**
1249 **timepoints (excel file, 7 tabs)**

1250 For each of the 7 patients with multiple biopsies, the clonal prevalence and
1251 evolutionary dynamic information is provided by depicting for each SNV
1252 (mutation_id) the cancer-cell fraction (cellular_prevalence) in each of the
1253 samples/time-point (sample_id), among other clone/cluster related information

1254

1255 **Supplemental Table 7. - IC50 Values for Drug Treatment Assays**

1256 Corresponding IC50 estimates to the various drug response relationships provide
1257 in Figure 4 and Supplemental Figures 4 and 5 are provided here

1258

1259 **Supplemental Table 8. - IC50 Values for Culture to Resistance Experiments**

1260 Corresponding IC50 estimates to the various drug response relationships
1261 provided in Figure 5 are provided here

1262

1263 **References**

1264 1. Spring, L.M., Wander, S.A., Zangardi, M. & Bardia, A. CDK 4/6 Inhibitors
1265 in Breast Cancer: Current Controversies and Future Directions. *Curr*
1266 *Oncol Rep* **21**, 25 (2019).

1267 2. Ballinger, T.J., Meier, J.B. & Jansen, V.M. Current Landscape of Targeted
1268 Therapies for Hormone-Receptor Positive, HER2 Negative Metastatic
1269 Breast Cancer. *Front Oncol* **8**, 308 (2018).

1270 3. Finn, R.S., *et al.* Palbociclib and Letrozole in Advanced Breast Cancer. *N*
1271 *Engl J Med* **375**, 1925-1936 (2016).

1272 4. Cristofanilli, M., *et al.* Fulvestrant plus palbociclib versus fulvestrant plus
1273 placebo for treatment of hormone-receptor-positive, HER2-negative
1274 metastatic breast cancer that progressed on previous endocrine therapy
1275 (PALOMA-3): final analysis of the multicentre, double-blind, phase 3
1276 randomised controlled trial. *Lancet Oncol* **17**, 425-439 (2016).

1277 5. Hortobagyi, G.N., *et al.* Ribociclib as First-Line Therapy for HR-Positive,
1278 Advanced Breast Cancer. *N Engl J Med* **375**, 1738-1748 (2016).

1279 6. Goetz, M.P., *et al.* MONARCH 3: Abemaciclib As Initial Therapy for
1280 Advanced Breast Cancer. *J Clin Oncol* **35**, 3638-3646 (2017).

1281 7. Sledge, G.W., Jr., *et al.* MONARCH 2: Abemaciclib in Combination With
1282 Fulvestrant in Women With HR+/HER2- Advanced Breast Cancer Who
1283 Had Progressed While Receiving Endocrine Therapy. *J Clin Oncol* **35**,
1284 2875-2884 (2017).

1285 8. Sledge, G.W., Jr., *et al.* The Effect of Abemaciclib Plus Fulvestrant on
1286 Overall Survival in Hormone Receptor-Positive, ERBB2-Negative Breast
1287 Cancer That Progressed on Endocrine Therapy-MONARCH 2: A
1288 Randomized Clinical Trial. *JAMA Oncol* (2019).

1289 9. Im, S.A., *et al.* Overall Survival with Ribociclib plus Endocrine Therapy in
1290 Breast Cancer. *N Engl J Med* **381**, 307-316 (2019).

1291 10. Dickler, M.N., *et al.* MONARCH 1, A Phase II Study of Abemaciclib, a
1292 CDK4 and CDK6 Inhibitor, as a Single Agent, in Patients with Refractory
1293 HR(+)/HER2(-) Metastatic Breast Cancer. *Clin Cancer Res* **23**, 5218-5224
1294 (2017).

1295 11. Finn, R.S., *et al.* PD 0332991, a selective cyclin D kinase 4/6 inhibitor,
1296 preferentially inhibits proliferation of luminal estrogen receptor-positive
1297 human breast cancer cell lines in vitro. *Breast Cancer Res* **11**, R77 (2009).

1298 12. Herrera-Abreu, M.T., *et al.* Early Adaptation and Acquired Resistance to
1299 CDK4/6 Inhibition in Estrogen Receptor-Positive Breast Cancer. *Cancer*
1300 *Res* **76**, 2301-2313 (2016).

1301 13. Condorelli, R., *et al.* Polyclonal RB1 mutations and acquired resistance to
1302 CDK 4/6 inhibitors in patients with metastatic breast cancer. *Ann Oncol*
1303 **29**, 640-645 (2018).

1304 14. O'Leary, B., *et al.* The Genetic Landscape and Clonal Evolution of Breast
1305 Cancer Resistance to Palbociclib plus Fulvestrant in the PALOMA-3 Trial.
1306 *Cancer Discov* **8**, 1390-1403 (2018).

1307 15. Fribbens, C., *et al.* Plasma ESR1 Mutations and the Treatment of
1308 Estrogen Receptor-Positive Advanced Breast Cancer. *J Clin Oncol* **34**,
1309 2961-2968 (2016).

1310 16. Tolaney, S.M., *et al.* Abstract 4458: Clinical significance of
1311 *PIK3CA* and *ESR1* mutations in ctDNA and FFPE
1312 samples from the MONARCH 2 study of abemaciclib plus fulvestrant.
1313 *Cancer Research* **79**, 4458-4458 (2019).

1314 17. Costa, C., *et al.* PTEN loss mediates clinical cross-resistance to CDK4/6
1315 and PI3Kalpha inhibitors in breast cancer. *Cancer Discov* (2019).

1316 18. Jansen, V.M., *et al.* Kinome-Wide RNA Interference Screen Reveals a
1317 Role for PDK1 in Acquired Resistance to CDK4/6 Inhibition in ER-Positive
1318 Breast Cancer. *Cancer Res* **77**, 2488-2499 (2017).

1319 19. Yang, C., *et al.* Acquired CDK6 amplification promotes breast cancer
1320 resistance to CDK4/6 inhibitors and loss of ER signaling and dependence.
1321 *Oncogene* **36**, 2255-2264 (2017).

1322 20. Caldron, C.E., *et al.* Cyclin E2 overexpression is associated with endocrine
1323 resistance but not insensitivity to CDK2 inhibition in human breast cancer
1324 cells. *Mol Cancer Ther* **11**, 1488-1499 (2012).

1325 21. Turner, N.C., *et al.* Cyclin E1 Expression and Palbociclib Efficacy in
1326 Previously Treated Hormone Receptor-Positive Metastatic Breast Cancer.
1327 *J Clin Oncol*, JCO1800925 (2019).

1328 22. Li, Z., *et al.* Loss of the FAT1 Tumor Suppressor Promotes Resistance to
1329 CDK4/6 Inhibitors via the Hippo Pathway. *Cancer Cell* **34**, 893-905 e898
1330 (2018).

1331 23. Cornell, L., Wander, S.A., Visal, T., Wagle, N. & Shapiro, G.I. MicroRNA-
1332 Mediated Suppression of the TGF-beta Pathway Confers Transmissible
1333 and Reversible CDK4/6 Inhibitor Resistance. *Cell Rep* **26**, 2667-2680
1334 e2667 (2019).

1335 24. Mao, P., *et al.* Acquired FGFR and FGF alterations confer resistance to
1336 estrogen receptor (ER) targeted therapy in ER+ metastatic breast cancer.
1337 *bioRxiv*, 605436 (2019).

1338 25. Nayar, U., *et al.* Acquired HER2 mutations in ER(+) metastatic breast
1339 cancer confer resistance to estrogen receptor-directed therapies. *Nat
1340 Genet* **51**, 207-216 (2019).

1341 26. Formisano, L., *et al.* Aberrant FGFR signaling mediates resistance to
1342 CDK4/6 inhibitors in ER+ breast cancer. *Nat Commun* **10**, 1373 (2019).

1343 27. Cohen, O., *et al.* Abstract S1-01: Whole exome and transcriptome
1344 sequencing of resistant ER+ metastatic breast cancer. *Cancer Research*
1345 **77**, S1-01-S01-01 (2017).

1346 28. Abba, M.C., *et al.* A Molecular Portrait of High-Grade Ductal Carcinoma In
1347 Situ. *Cancer Res* **75**, 3980-3990 (2015).

1348 29. Zehir, A., *et al.* Mutational landscape of metastatic cancer revealed from
1349 prospective clinical sequencing of 10,000 patients. *Nat Med* **23**, 703-713
1350 (2017).

1351 30. Jeselsohn, R., Buchwalter, G., De Angelis, C., Brown, M. & Schiff, R.

1352 ESR1 mutations-a mechanism for acquired endocrine resistance in breast

1353 cancer. *Nat Rev Clin Oncol* **12**, 573-583 (2015).

1354 31. Tate, J.G., *et al.* COSMIC: the Catalogue Of Somatic Mutations In Cancer.

1355 *Nucleic Acids Res* **47**, D941-D947 (2019).

1356 32. Marchio, C., *et al.* The genetic landscape of breast carcinomas with

1357 neuroendocrine differentiation. *J Pathol* **241**, 405-419 (2017).

1358 33. Bessiere, L., *et al.* A Hot-spot of In-frame Duplications Activates the

1359 Oncoprotein AKT1 in Juvenile Granulosa Cell Tumors. *EBioMedicine* **2**,

1360 421-431 (2015).

1361 34. Gong, X., *et al.* Aurora A Kinase Inhibition Is Synthetic Lethal with Loss of

1362 the RB1 Tumor Suppressor Gene. *Cancer Discov* **9**, 248-263 (2019).

1363 35. Etemadmoghadam, D., *et al.* Synthetic lethality between CCNE1

1364 amplification and loss of BRCA1. *Proc Natl Acad Sci U S A* **110**, 19489-

1365 19494 (2013).

1366 36. Drago, J.Z., *et al.* FGFR1 gene amplification mediates endocrine

1367 resistance but retains TORC sensitivity in metastatic hormone receptor

1368 positive (HR+) breast cancer. *Clin Cancer Res* (2019).

1369 37. Karnitz, L.M. & Zou, L. Molecular Pathways: Targeting ATR in Cancer

1370 Therapy. *Clin Cancer Res* **21**, 4780-4785 (2015).

1371 38. Sakurikar, N., Thompson, R., Montano, R. & Eastman, A. A subset of

1372 cancer cell lines is acutely sensitive to the Chk1 inhibitor MK-8776 as

1373 monotherapy due to CDK2 activation in S phase. *Oncotarget* **7**, 1380-
1374 1394 (2016).

1375 39. Hong, D., *et al.* Phase I Study of LY2606368, a Checkpoint Kinase 1
1376 Inhibitor, in Patients With Advanced Cancer. *J Clin Oncol* **34**, 1764-1771
1377 (2016).

1378 40. Willems, E., *et al.* The functional diversity of Aurora kinases: a
1379 comprehensive review. *Cell Div* **13**, 7 (2018).

1380 41. Staff, S., Isola, J., Jumppanen, M. & Tanner, M. Aurora-A gene is
1381 frequently amplified in basal-like breast cancer. *Oncol Rep* **23**, 307-312
1382 (2010).

1383 42. Opyrchal, M., *et al.* Aurora-A mitotic kinase induces endocrine resistance
1384 through down-regulation of ERalpha expression in initially ERalpha+
1385 breast cancer cells. *PLoS One* **9**, e96995 (2014).

1386 43. Haddad, T.C., *et al.* Phase I trial to evaluate the addition of alisertib to
1387 fulvestrant in women with endocrine-resistant, ER+ metastatic breast
1388 cancer. *Breast Cancer Res Treat* **168**, 639-647 (2018).

1389 44. Oser, M.G., *et al.* Cells Lacking the RB1 Tumor Suppressor Gene Are
1390 Hyperdependent on Aurora B Kinase for Survival. *Cancer Discov* **9**, 230-
1391 247 (2019).

1392 45. Chakravarty, D., *et al.* OncoKB: A Precision Oncology Knowledge Base.
1393 *JCO Precis Oncol* **2017**(2017).

1394 46. Sondka, Z., *et al.* The COSMIC Cancer Gene Census: describing genetic
1395 dysfunction across all human cancers. *Nat Rev Cancer* **18**, 696-705
1396 (2018).

1397 47. Sanchez-Vega, F., *et al.* Oncogenic Signaling Pathways in The Cancer
1398 Genome Atlas. *Cell* **173**, 321-337 e310 (2018).

1399 48. Vogelstein, B., *et al.* Cancer genome landscapes. *Science* **339**, 1546-
1400 1558 (2013).

1401 49. Adalsteinsson, V.A., *et al.* Scalable whole-exome sequencing of cell-free
1402 DNA reveals high concordance with metastatic tumors. *Nat Commun* **8**,
1403 1324 (2017).

1404 50. Fisher, S., *et al.* A scalable, fully automated process for construction of
1405 sequence-ready human exome targeted capture libraries. *Genome Biol*
1406 **12**, R1 (2011).

1407 51. Reich, M., *et al.* GenePattern 2.0. *Nat Genet* **38**, 500-501 (2006).

1408 52. Cibulskis, K., *et al.* ContEst: estimating cross-contamination of human
1409 samples in next-generation sequencing data. *Bioinformatics* **27**, 2601-
1410 2602 (2011).

1411 53. Cibulskis, K., *et al.* Sensitive detection of somatic point mutations in
1412 impure and heterogeneous cancer samples. *Nat Biotechnol* **31**, 213-219
1413 (2013).

1414 54. Saunders, C.T., *et al.* Strelka: accurate somatic small-variant calling from
1415 sequenced tumor-normal sample pairs. *Bioinformatics* **28**, 1811-1817
1416 (2012).

1417 55. Costello, M., *et al.* Discovery and characterization of artifactual mutations
1418 in deep coverage targeted capture sequencing data due to oxidative DNA
1419 damage during sample preparation. *Nucleic Acids Res* **41**, e67 (2013).

1420 56. Van Allen, E.M., *et al.* Whole-exome sequencing and clinical interpretation
1421 of formalin-fixed, paraffin-embedded tumor samples to guide precision
1422 cancer medicine. *Nat Med* **20**, 682-688 (2014).

1423 57. Ramos, A.H., *et al.* Oncotator: cancer variant annotation tool. *Hum Mutat*
1424 **36**, E2423-2429 (2015).

1425 58. Olshen, A.B., Venkatraman, E.S., Lucito, R. & Wigler, M. Circular binary
1426 segmentation for the analysis of array-based DNA copy number data.
1427 *Biostatistics* **5**, 557-572 (2004).

1428 59. DePristo, M.A., *et al.* A framework for variation discovery and genotyping
1429 using next-generation DNA sequencing data. *Nat Genet* **43**, 491-498
1430 (2011).

1431 60. Wala, J.A., *et al.* SvABA: genome-wide detection of structural variants and
1432 indels by local assembly. *Genome Res* **28**, 581-591 (2018).

1433 61. Walsh, R., *et al.* Reassessment of Mendelian gene pathogenicity using
1434 7,855 cardiomyopathy cases and 60,706 reference samples. *Genet Med*
1435 **19**, 192-203 (2017).

1436 62. Carter, S.L., *et al.* Absolute quantification of somatic DNA alterations in
1437 human cancer. *Nat Biotechnol* **30**, 413-421 (2012).

1438 63. Roth, A., *et al.* PyClone: statistical inference of clonal population structure
1439 in cancer. *Nat Methods* **11**, 396-398 (2014).

1440 64. Dang, H.X., *et al.* ClonEvol: clonal ordering and visualization in cancer

1441 sequencing. *Ann Oncol* **28**, 3076-3082 (2017).

1442 65. Ulz, P., *et al.* Whole-genome plasma sequencing reveals focal

1443 amplifications as a driving force in metastatic prostate cancer. *Nat*

1444 *Commun* **7**, 12008 (2016).

1445

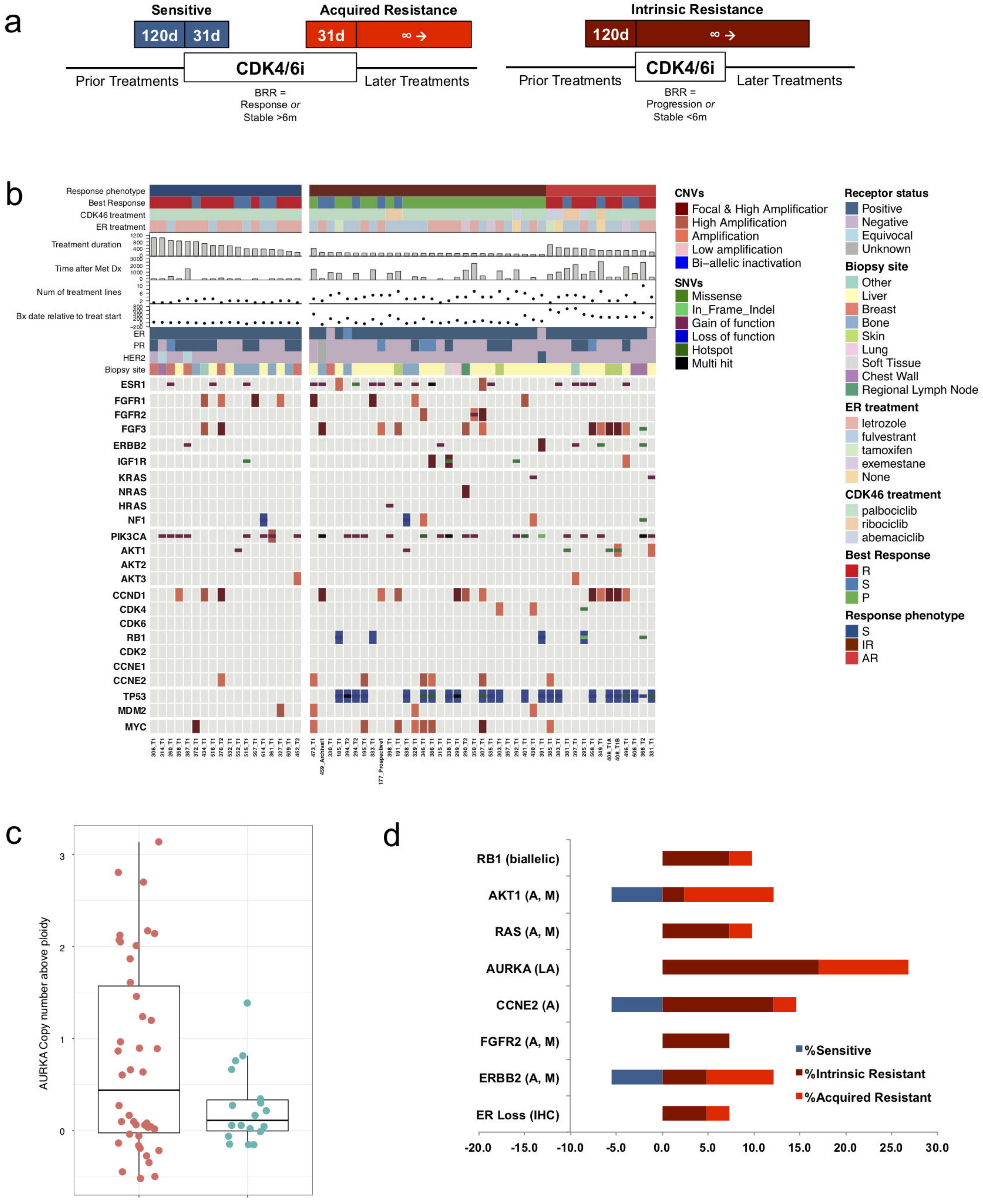


Figure 1. The genomic landscape of CDK4/6i resistance is heterogeneous, with multiple potential driver events.

(a) Biopsy phenotypes were assigned as *sensitive*, *acquired resistance*, or *intrinsic resistance* based upon timing of the biopsy relative to CDK4/6i exposure (d - days), best radiographic response (BRR), and duration of treatment. Patients were categorized as experiencing clinical benefit on CDK4/6i if interval restaging demonstrated a response or disease stability for at least six months. (b) Mutational matrix (CoMut) depicting the genomic landscape of the CDK4/6i cohort (n = 59 biopsies, 58 patients). Copy number alterations and mutational events in select genes of interest are shown. Clinical parameters (shown at the top) include receptor status, anti-estrogen agent, CDK4/6 inhibitor, best radiographic response (P – progression, R – response, S – stable), biopsy phenotype (S – sensitive, IR – intrinsic resistance, AR – acquired resistance), treatment duration (days), biopsy timing relative to treatment initiation (days), time since metastatic diagnosis (days), and number of lines of prior treatment. (c) Phenotype distribution plot demonstrating a higher frequency of copy number amplifications in Aurora Kinase A (AURKA) among resistant biopsies (AR + IR, left) compared to sensitive biopsies (right, 0.0081, Welch test). (d) Bar plot visualization of mutational (M) and/or copy number alterations (A – amplification, LA – low amplification) in select genes. The proportional enrichment (fraction of samples demonstrating alteration) in sensitive biopsies (left, blue) and resistant biopsies (AR + IR, right, red) is included.

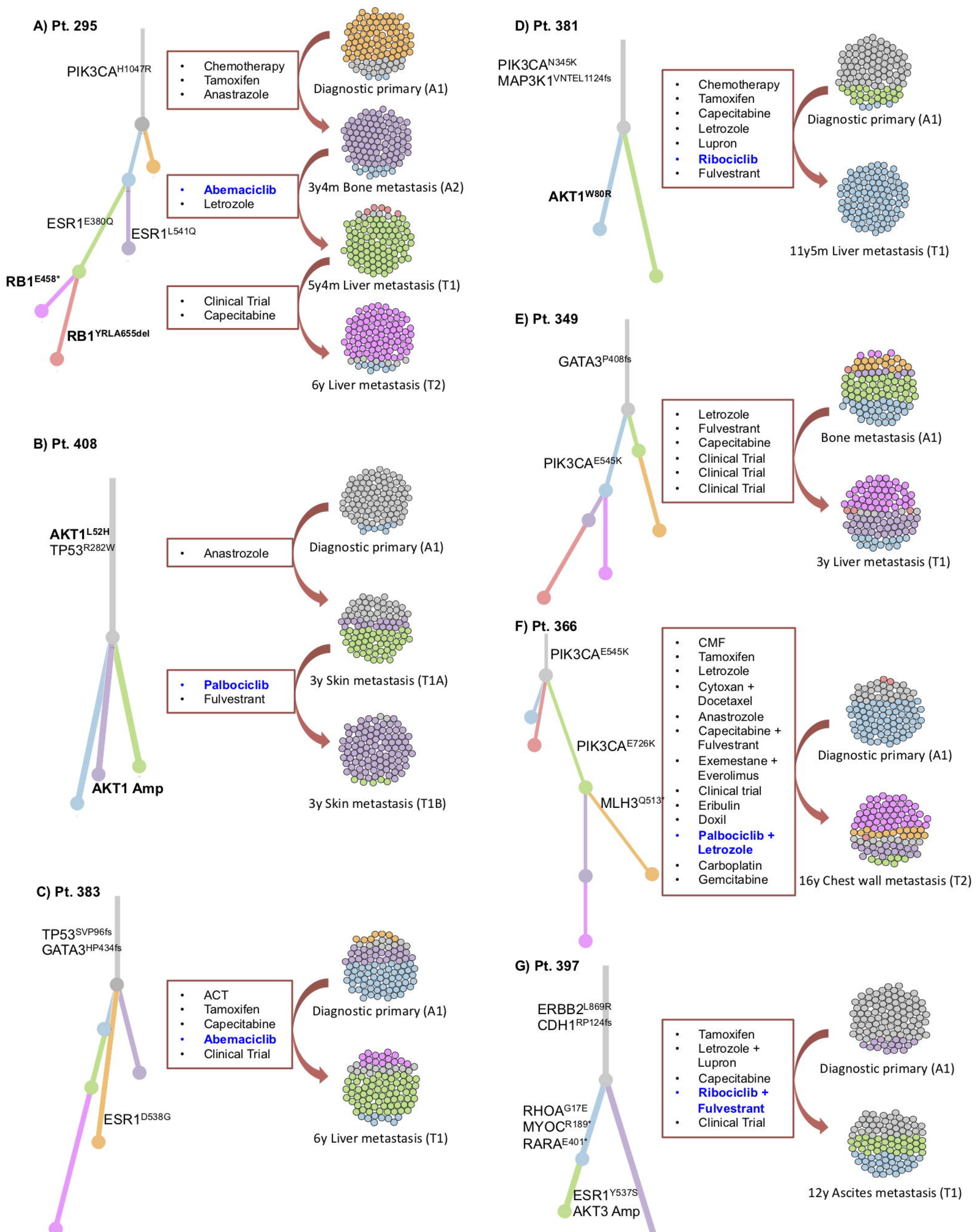
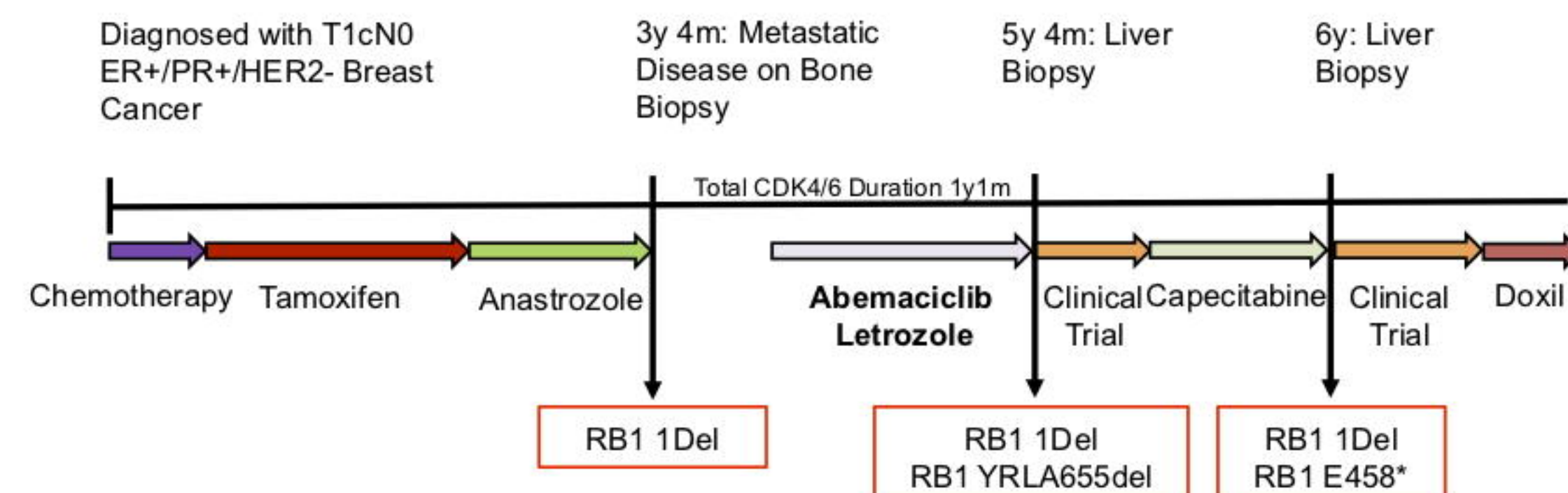
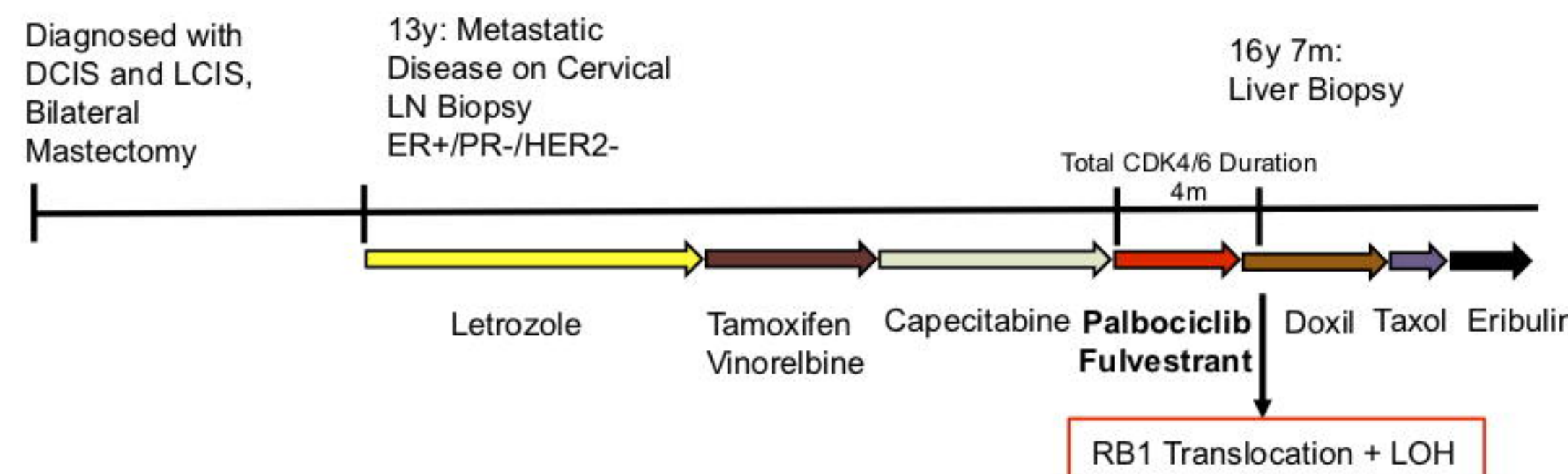
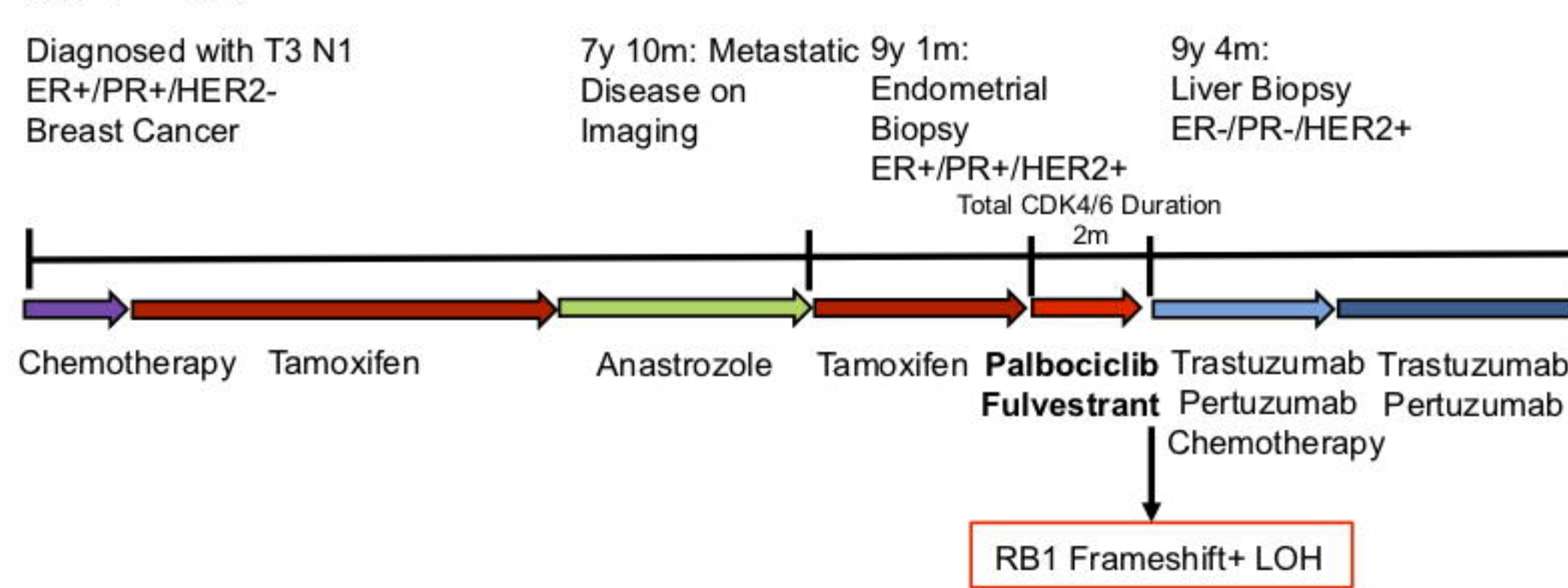
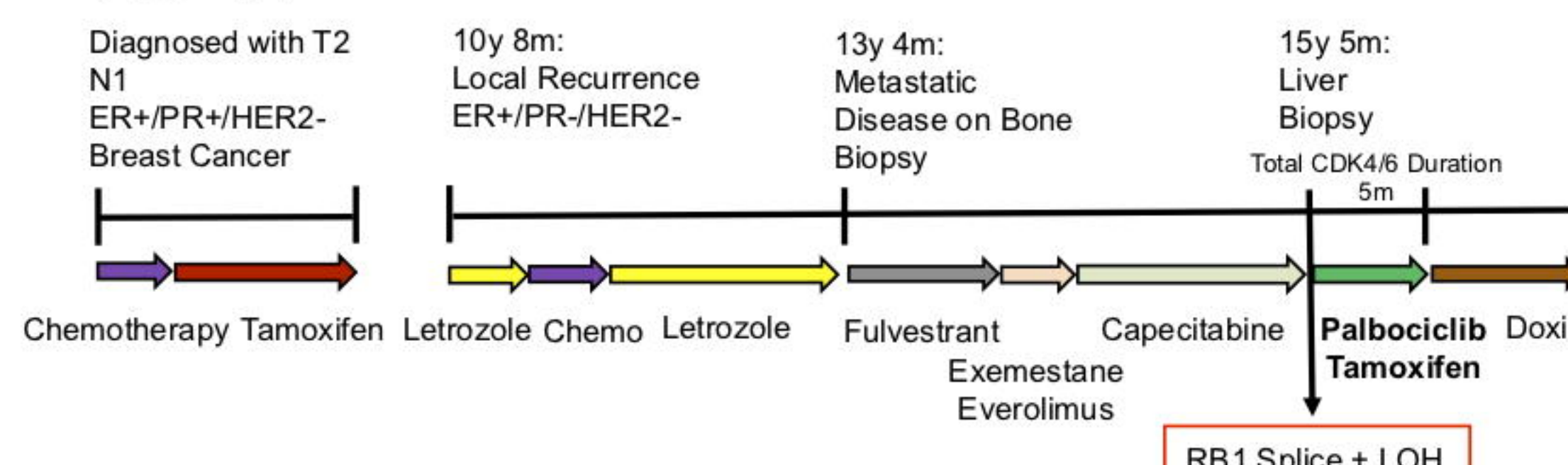
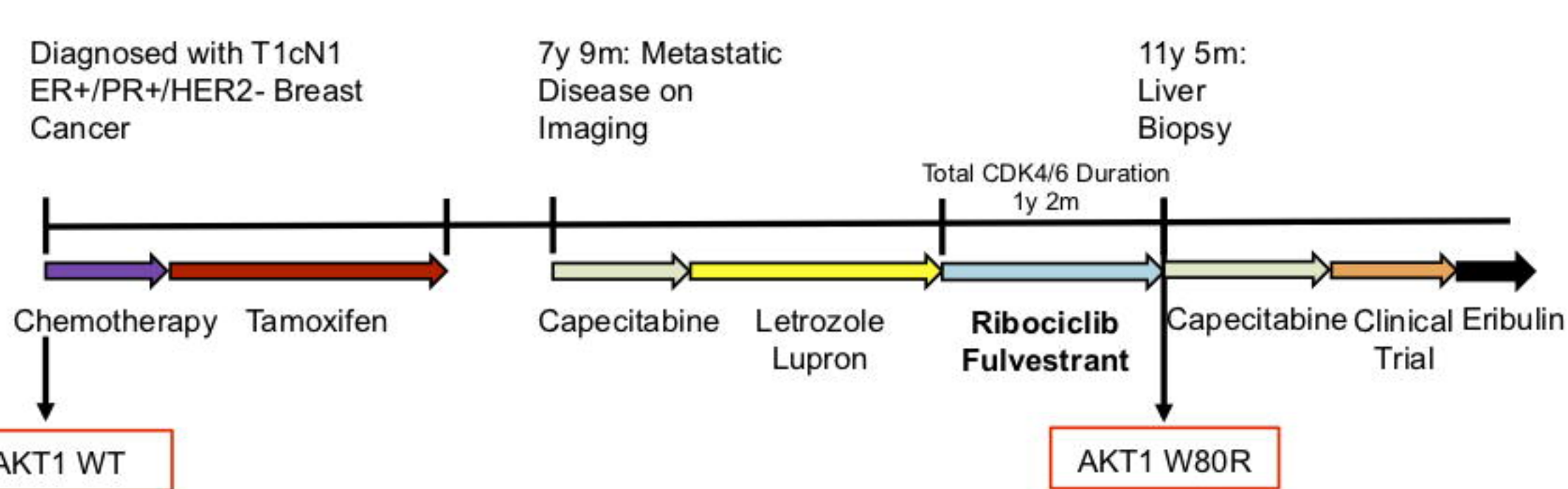
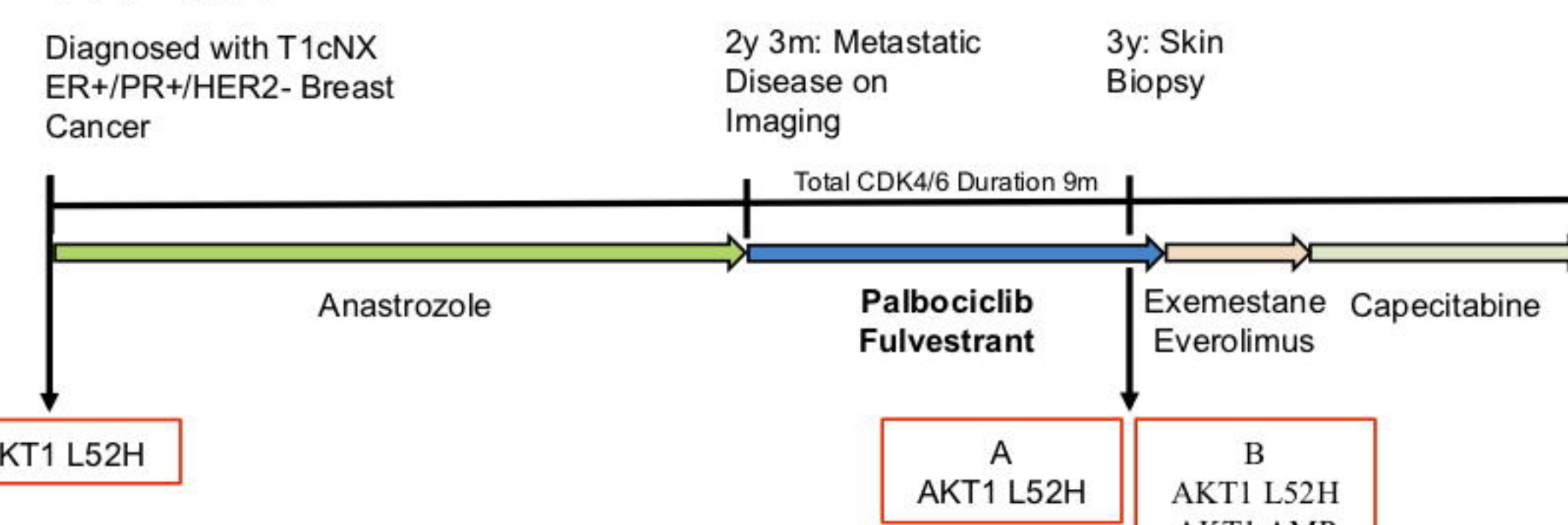
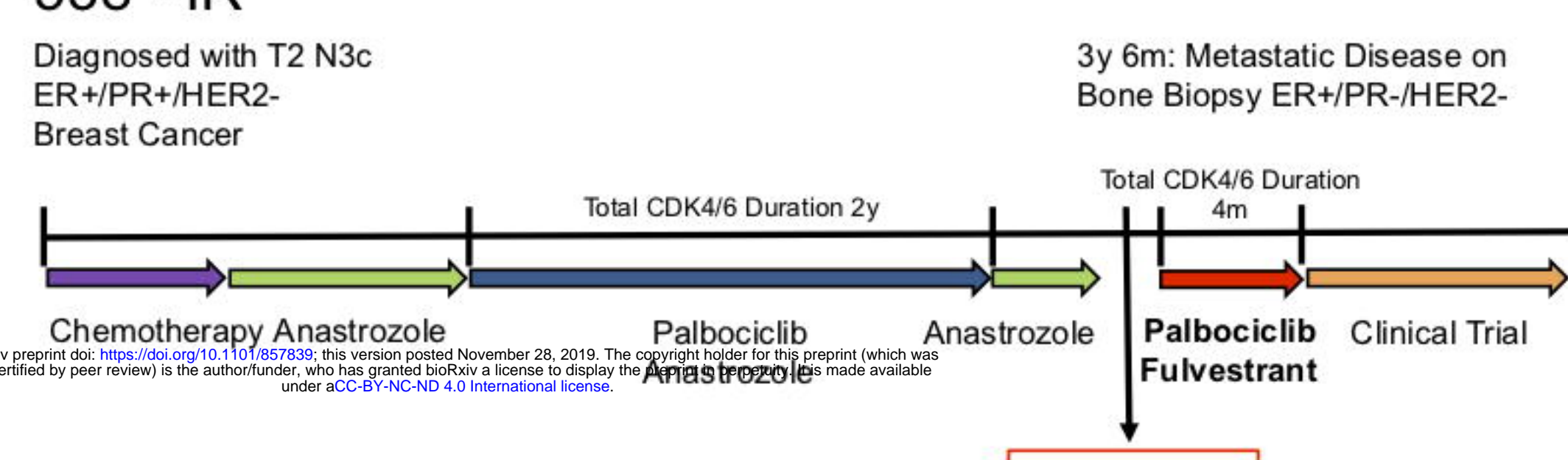
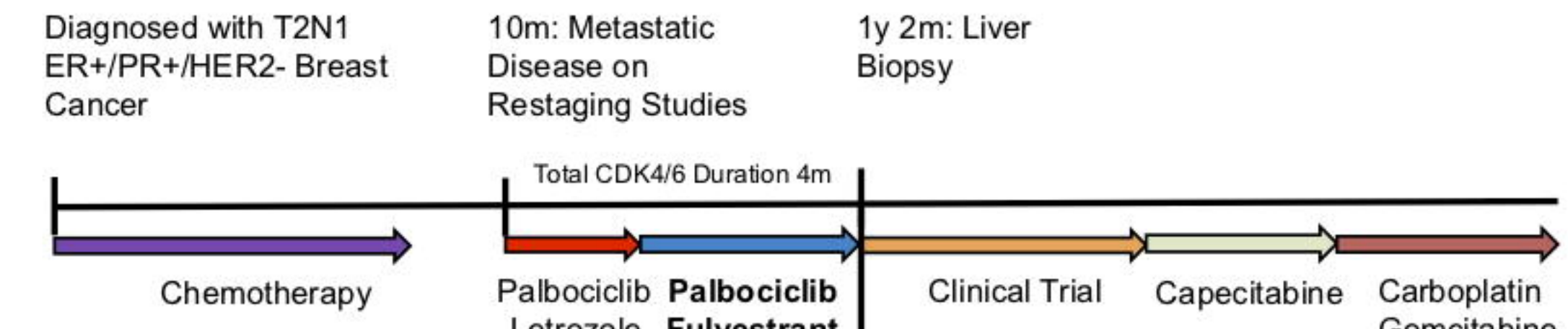
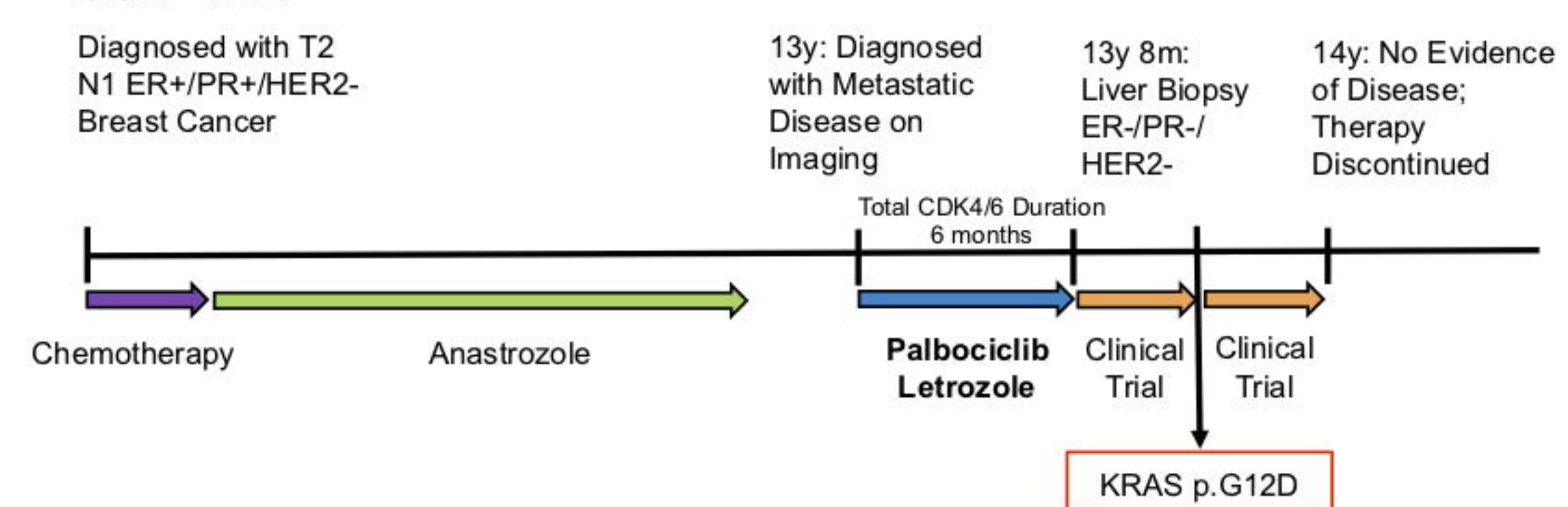
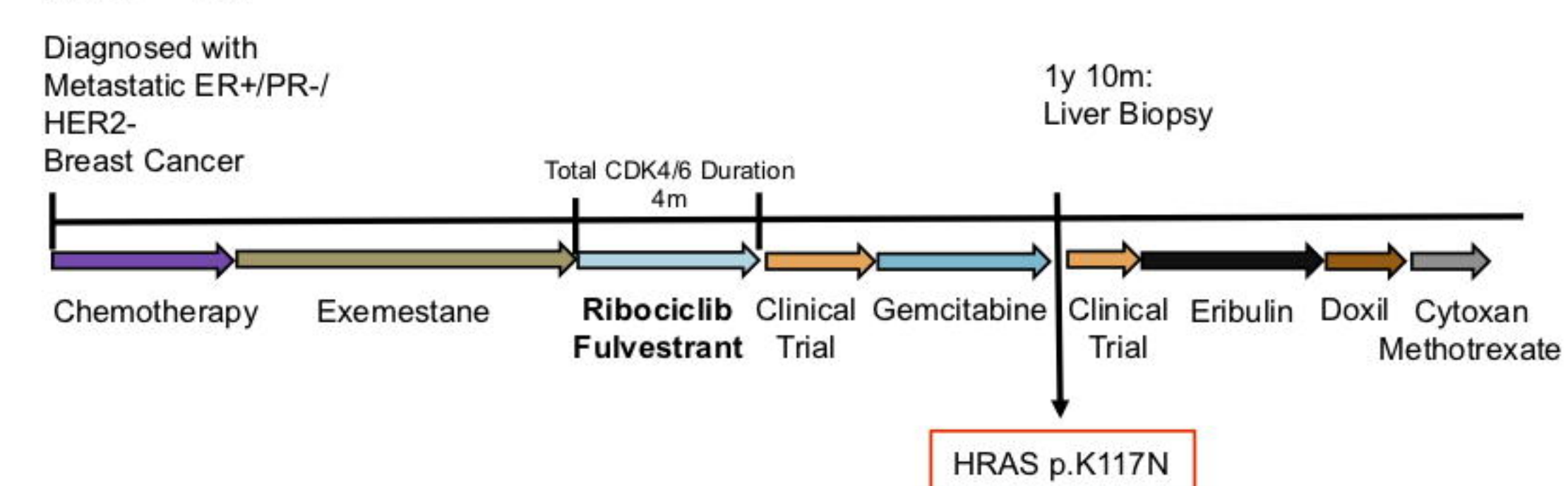
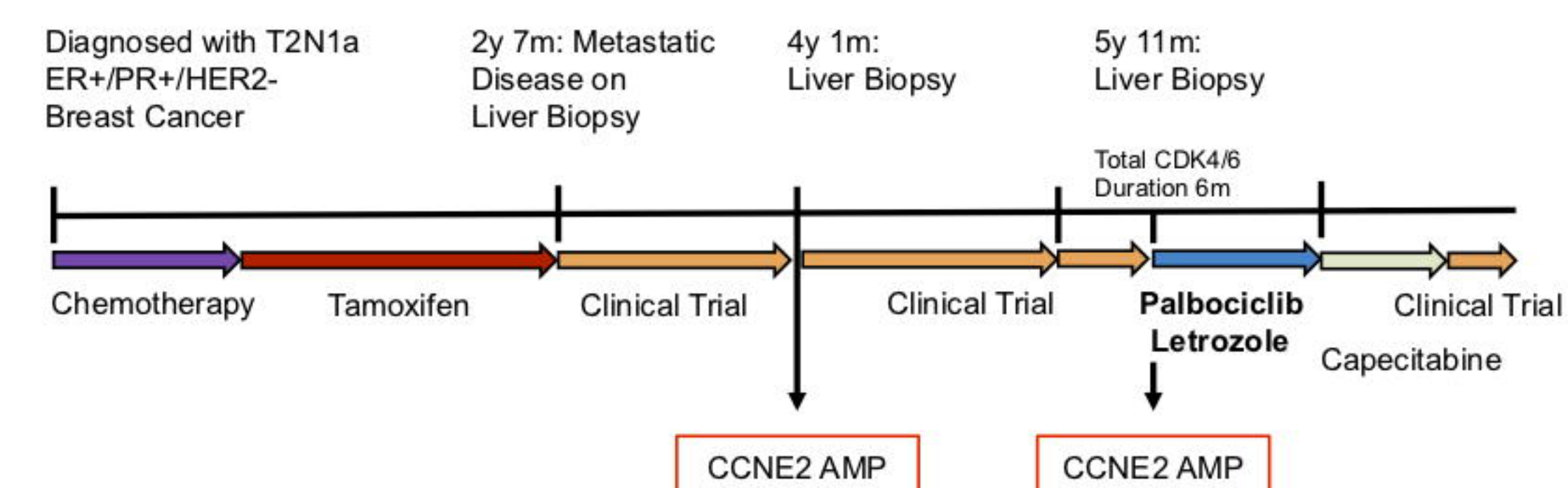
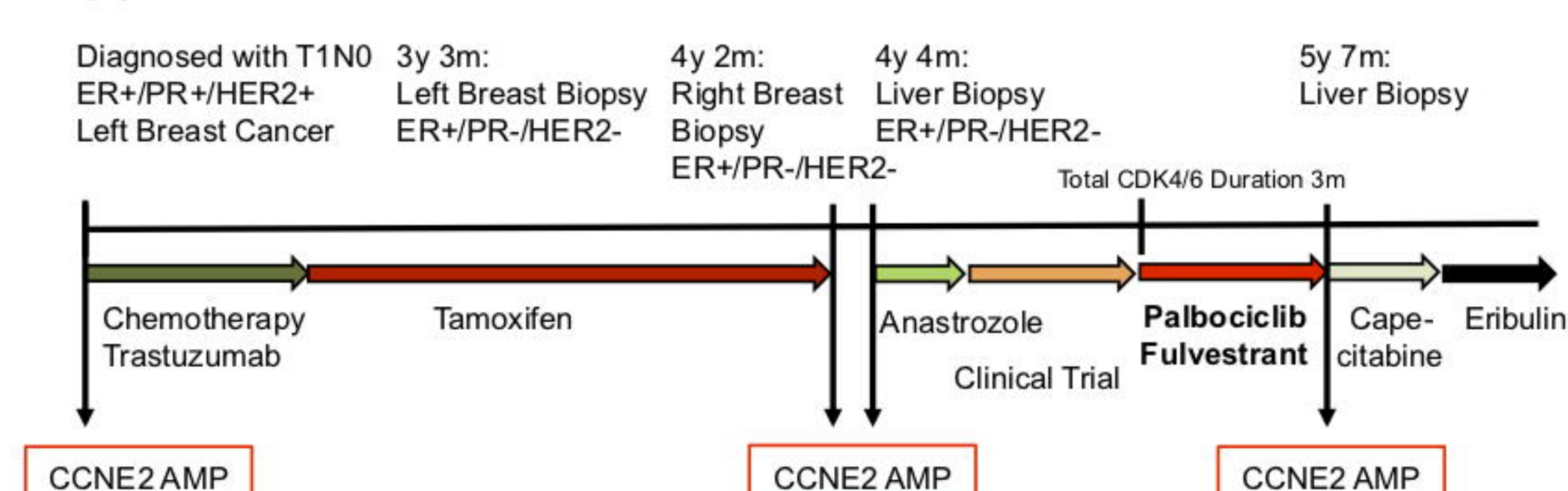
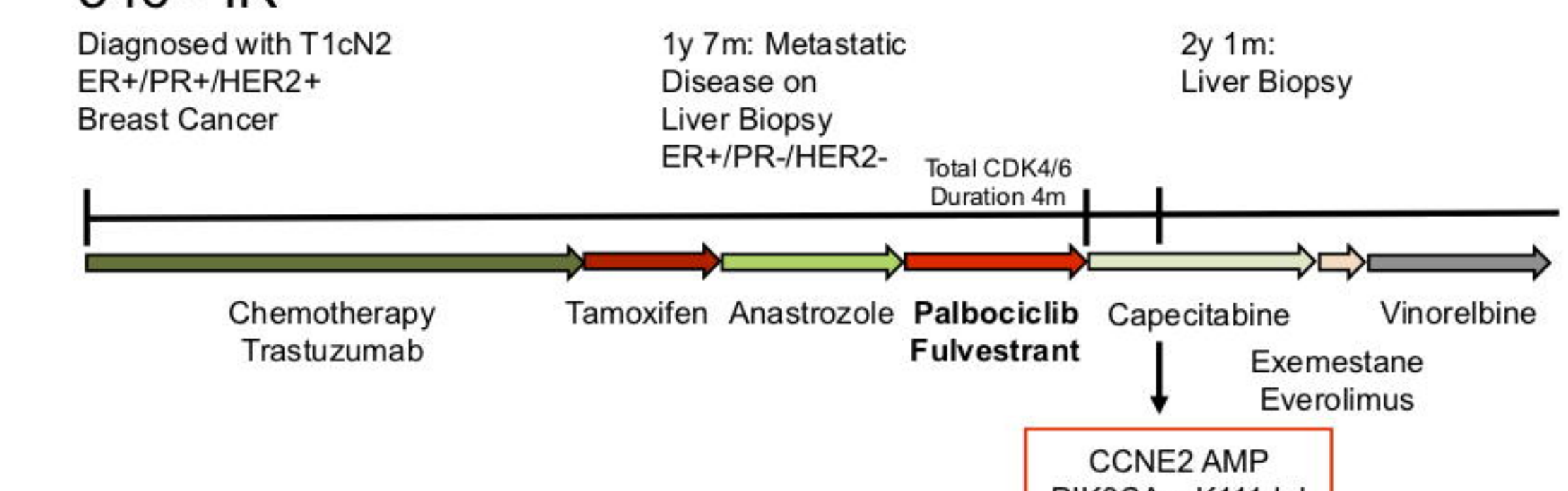
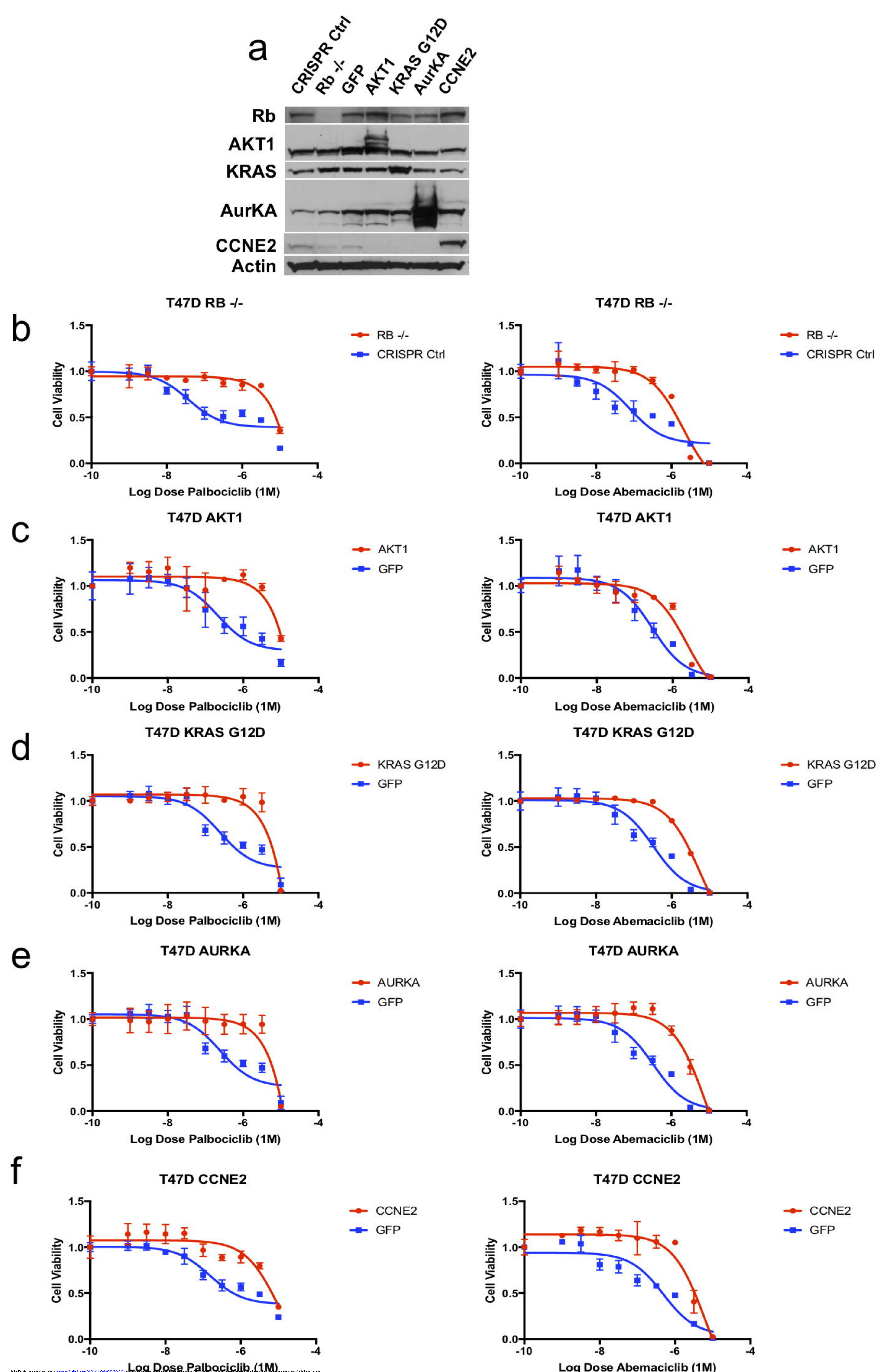


Figure 2. Acquired resistance to CDK4/6i in patients with pre-treatment and post-progression biopsies demonstrates convergent evolution of biallelic RB1 disruption and evolved AKT1 activation.

Phylogenetic analysis depicting the evolutionary history for seven patients with acquired alterations, with clonal evolutionary dynamics demonstrating: (a) acquired polyclonal ESR1 mutations after aromatase inhibition, followed by convergent evolution of RB1 inactivation, with different RB1-inactivating mutations acquired in two parallel sibling clones; (b) Acquired AKT1 amplification; (c) No notable candidate for acquired mechanism of resistance (MOR); (d) Acquired AKT1 (W80R) mutation; (e) No notable candidate for acquired MOR; (f) Acquired inactivation of DNA Mismatch Repair Protein (MLH3); and (g) Acquired activating ESR1 mutation (Y537S) and amplification in AKT3.

a 295 - AR**333 - IR****391 - IR****185 - IR****b****381 - AR****408 - AR****538 - IR****C 430 - IR****331 - AR****398 - IR****195 - IR****307 - IR****346 - IR****Figure 3. Clinical vignettes for candidate resistance drivers in representative patients (RB1, AKT1, RAS, and CCNE2).**

Clinical vignettes including treatment sequence, timing of metastatic progression, and available biopsies with key genomic findings are provided for the following - (a) four patients with biallelic alterations in RB1, including a patient with multiple biopsies and convergent evolution toward RB1 disruption (top, phylogenetic analysis for this patient is provided in Figure 2A). (b) Three patients with acquired alterations in AKT1 following progression on CDK4/6i. In the first (top), a new mutation in AKT1 W80R was identified. In the second (middle), a baseline alteration (AKT1 L52H) was identified at the time of diagnosis; at the time of progression on CDK4/6i, two biopsies were obtained – both demonstrating the baseline AKT1 L52H mutation, one also demonstrating an acquired amplification of the wild-type AKT1 protein (phylogenetic analyses for these patients are provided in Figure 2B and D). (c) Three patients with resistance to CDK4/6i and RAS-family alterations (including two instances of KRAS G12D and one instance of HRAS mutation). (d) Three patients with intrinsic resistance to CDK4/6i and amplification events in CCNE2.



bioRxiv preprint doi: <https://doi.org/10.1101/857839>; this version posted April 2, 2018. The copyright holder for this preprint (which was not certified by peer review) is the author/funder, who has granted bioRxiv a license to display the preprint in perpetuity. It is made available under aCC-BY-NC-ND 4.0 International license.

Figure 4. Candidate genomic alterations provoke CDK4/6i resistance *in vitro*.

(a) T47D cells were modified via CRISPR-mediated downregulation (RB1) or lentiviral overexpression (AKT1, KRAS G12D, AURKA, CCNE2) to interrogate potential resistance mediators identified in patient biopsy samples. Western blotting with the indicated antibodies is included. (b-f) Modified T47D cells were exposed to escalating doses of CDK4/6i (palbociclib – left, abemaciclib – right) and viability was estimated via cell-titer-glo (CTG) assay. Control (CRISPR non-targeting guide or GFP) cells are plotted along with the resistance driver of interest (RB1 – b, AKT1 – c, KRAS G12D – d, AURKA – e, CCNE2 – f). Parental and variant cell lines are normalized to vehicle control and viability is plotted as a function of increasing CDK4/6i (graphed as triplicate average +/- standard deviation). All variants provoke CDK4/6i resistance (to both palbociclib and abemaciclib) *in vitro* in T47D cells. Corresponding IC₅₀ values are included in Supplemental Table 7.

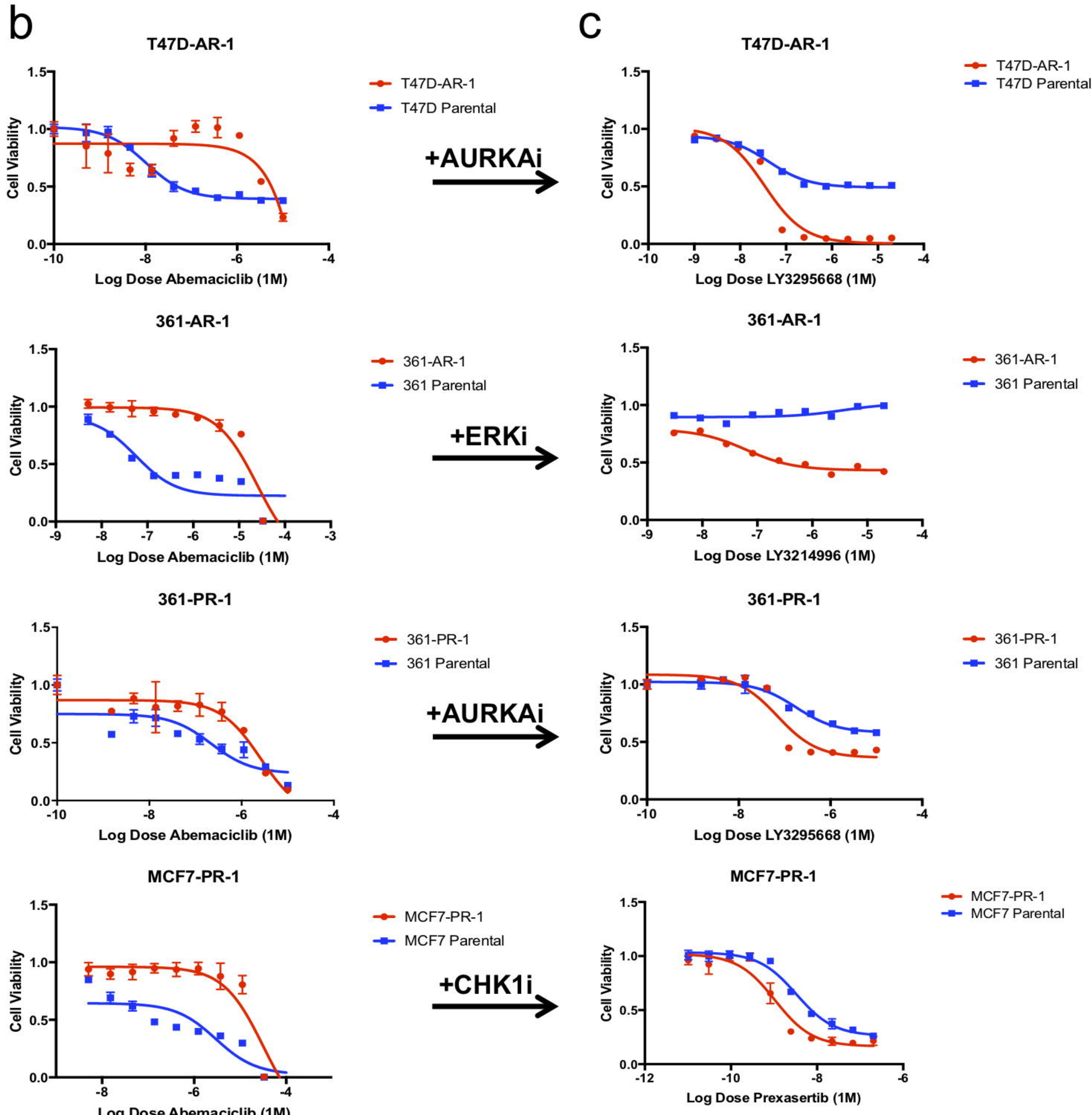
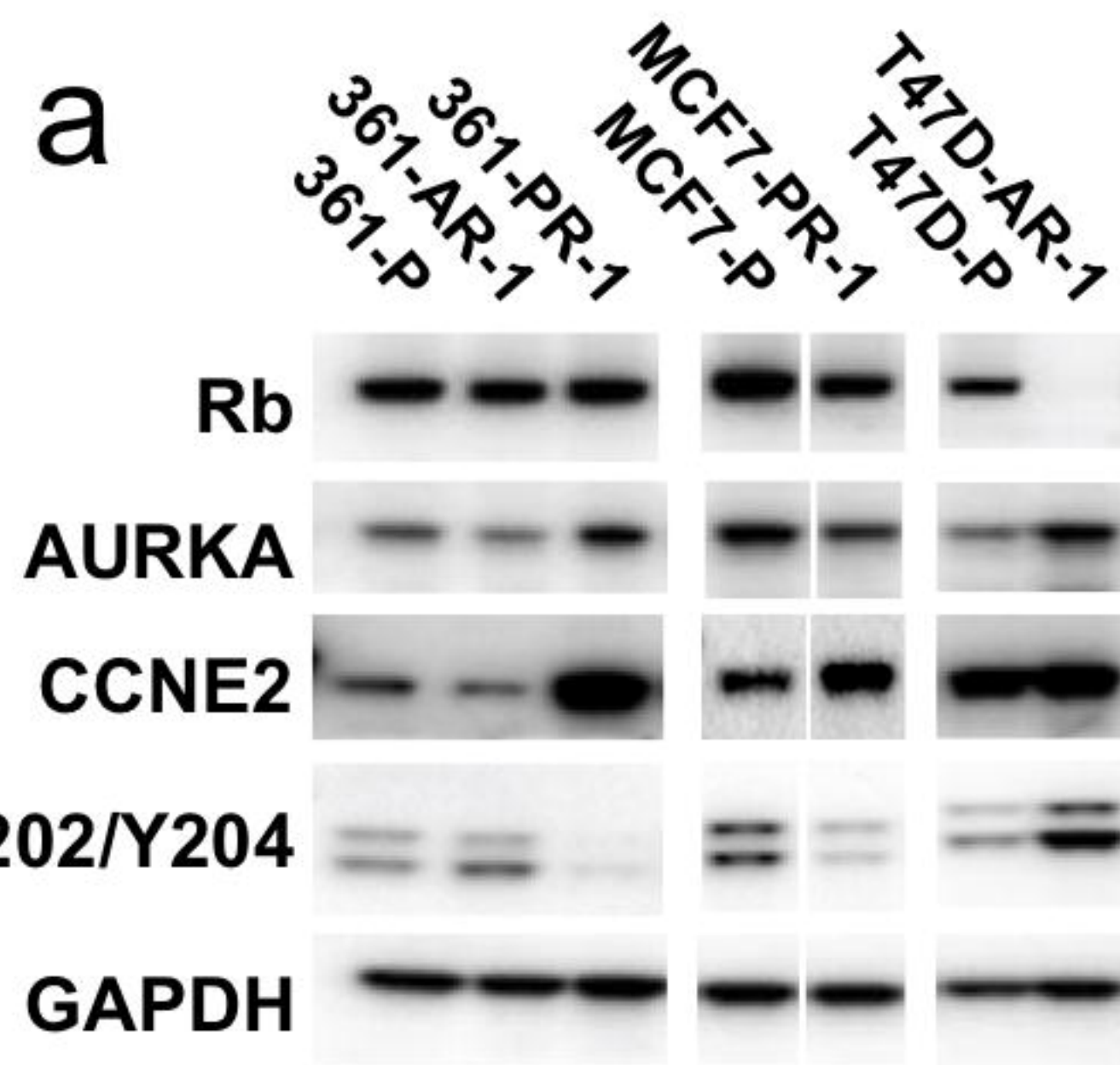


Figure 5. Candidate mutations emerge in cell lines cultured under CDK4/6i selective pressure and define new therapeutic dependencies *in vitro*.

bioRxiv preprint doi: <https://doi.org/10.1101/857839>; this version posted November 28, 2019. The copyright holder for this preprint (which was not certified by peer review) is the author/funder, who has granted bioRxiv a license to display the preprint in perpetuity. It is made available under aCC-BY-NC-ND 4.0 International license.

(a) Breast cancer cell lines (T47D, MCF7, MDA-MB-361) were cultured long-term to resistance in the presence of CDK4/6i (palbociclib, abemaciclib). The resulting cell lines which emerged were subjected to western blotting for putative mediators of drug resistance (RB1, AKT1, KRAS/ERK, AURKA, and CCNE2). (b-c) T47D cells cultured to resistance in the presence of abemaciclib demonstrated low levels of RB1 expression (T47D-AR1) and increased sensitivity to the AURKA inhibitor LY3295668. MDA-MB-361 cells cultured to resistance in the presence of abemaciclib demonstrated high levels of ERK activation (361-AR1) and increased sensitivity to the ERK inhibitor LY3214996. MDA-MB-361 cells cultured to resistance in the presence of palbociclib demonstrated high levels of AURKA (361-PR1) and increased sensitivity to the AURKA inhibitor LY3295668. MCF7 cells cultures to resistance in the presence of palbociclib demonstrated increased levels of CCNE2 (MCF7-PR1) and increased sensitivity to the CHEK1 inhibitor prexasertib.

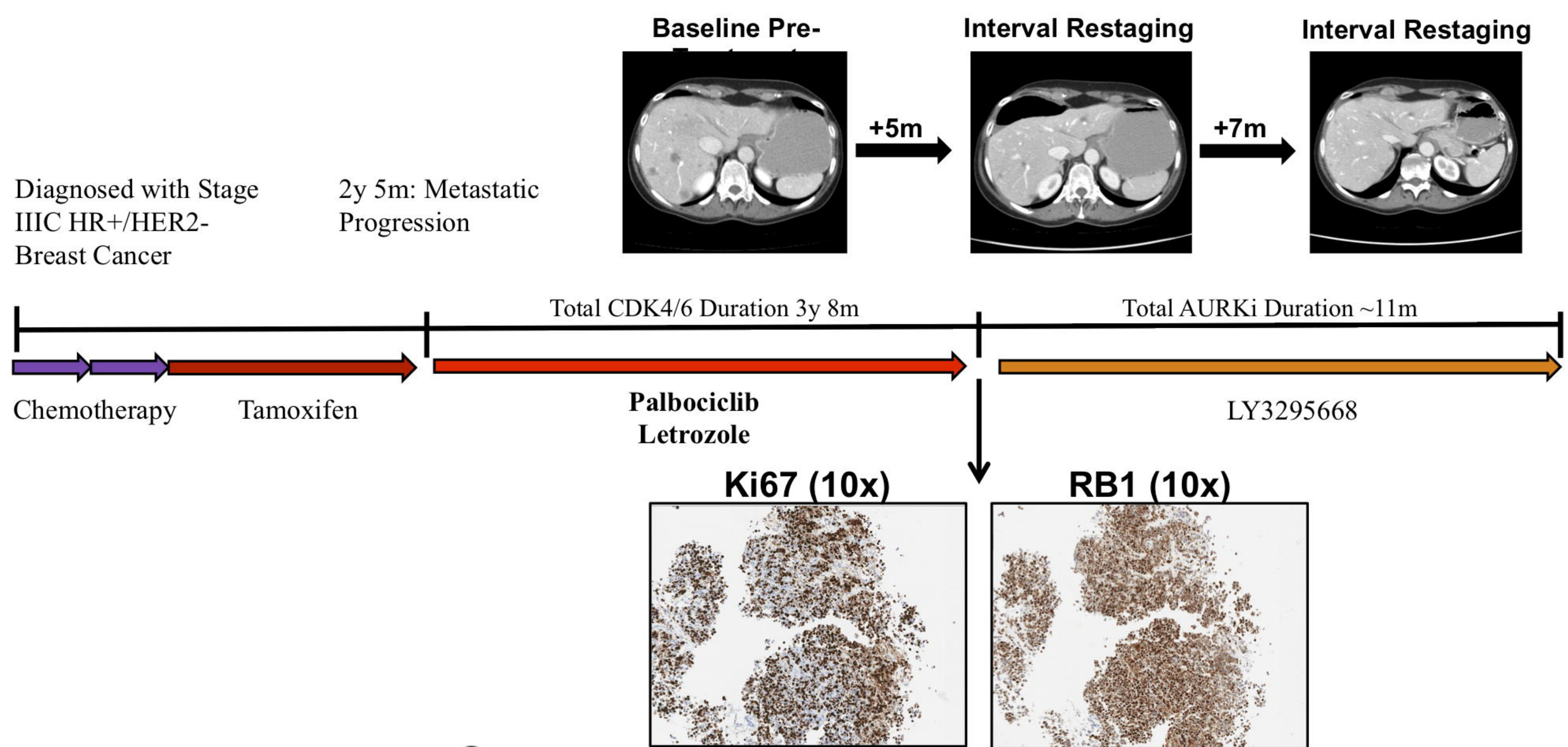
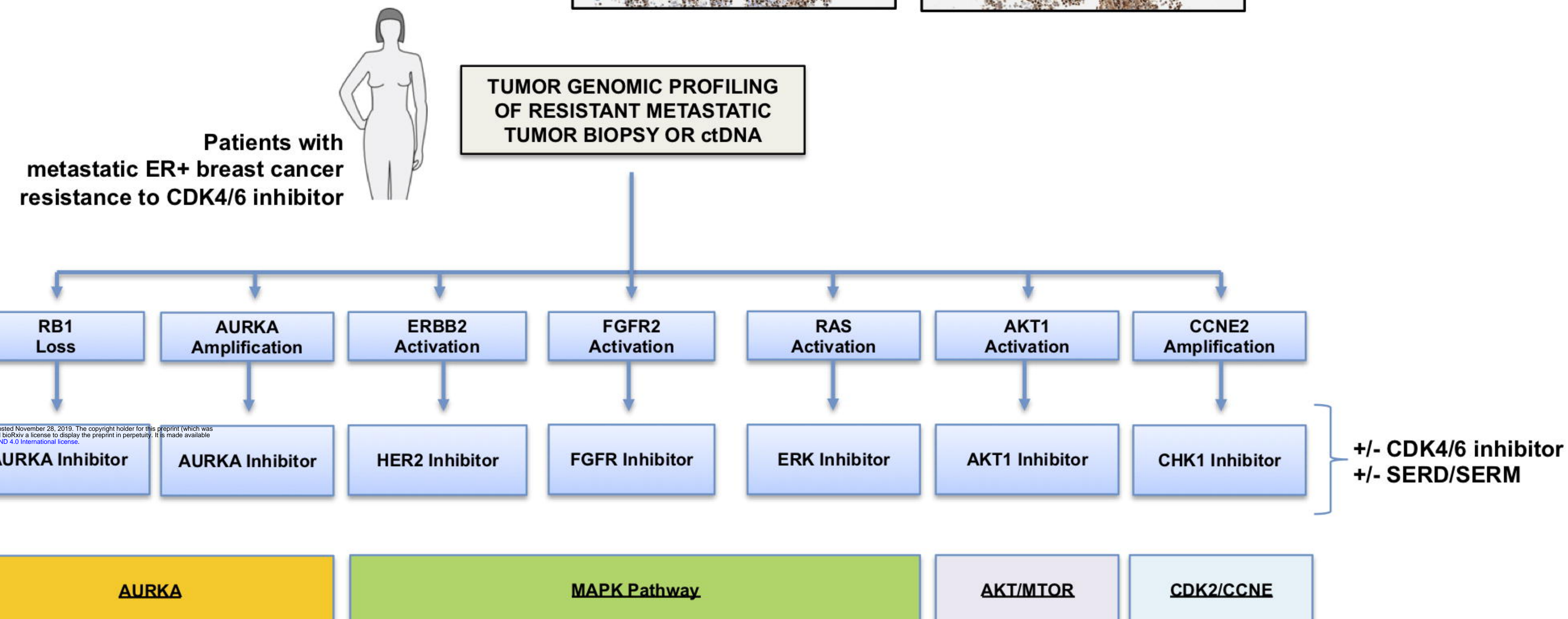
a**b**

Figure 6. A novel aurora kinase A inhibitor demonstrates therapeutic efficacy in a patient with metastatic HR+ breast cancer after progression on CDK4/6i.

(a) A patient with locally advanced HR+/HER2- breast cancer developed metastatic progression on adjuvant tamoxifen. She received CDK4/6i and letrozole in the first line setting with prolonged clinical benefit (>3 years). At progression, she was placed on trial with the AURKA inhibitor LY3295668; she subsequently experienced prolonged disease control (~11 months). Baseline staging studies following progression on CDK4/6i in the patient described are included (top); she had osseous metastatic disease and visceral disease was limited to the foci noted in the liver. Two interval restaging studies (top) demonstrate disease stability/mild response. Liver biopsy obtained at the time of progression on CDK4/6i and prior to LY3295668 demonstrated high Ki67 and high RB1 protein expression via immunohistochemistry (IHC, 10x) (bottom). (b) Schematic diagram demonstrating the potential utility of next-generation sequencing following progression on CDK4/6i; actionable alterations in RB1, ERBB2, FGFR2, AKT1, RAS, AURKA, and CCNE2 could dictate informed selection of targeted therapies as indicated.